Minimum-Noise-Variance Beamformer with an Electromagnetic Vector Sensor

Arye Nehorai, *Fellow, IEEE,* Kwok-Chiang Ho, and B. T. G. Tan

***Abstract*— We study the performance of the minimum-noise-variance beamformer employing a single electromagnetic (EM) vector sensor that is capable of measuring the complete electric and magnetic fields induced by EM signals at one point. Two types of signals are considered: One carries a single message, and the other carries two independent messages simultaneously. The state of polarization of the interference under consideration ranges from completely polarized to unpolarized. We first obtain explicit expressions for the signal to interference-plus-noise ratio (SINR) in terms of the parameters of the signal, interference, and noise. Then, we discuss some physical implications associated with the SINR expressions. These expressions provide a basis for effective interference suppression as well as generation of dual-message signals of which the two message signals have minimum interference effect on one another. We also analyze the characteristics of the main-lobe and side-lobe of the beampattern of an EM vector sensor and compare them with other types of sensor arrays.**

***Index Terms*— Beamformer, direction of arrival, electromagnetic, vector sensor.**

I. Introduction

DIRECTION-of-arrival (DOA) estimation and beamforming for electromagnetic (EM) waves are two common objectives of array processing. Early work on DOA estimation and beamforming has been based on scalar sensors, each of which provides measurements of only one component of the electric or magnetic field induced [18]. Subsequent research has investigated the use of sensors that measure two components of the electric or magnetic field (see, e.g., [19]–[21]) and tripole sensors that measure three complete components of the electric field [22]. In recent years, researchers have proposed the use of EM vector sensors that measure the three complete components of the electric field and three components of the magnetic field at one point for DOA estimation [1]–[17].

EM vector sensors as measuring devices are commercially available and actively researched. Indeed, EMC Baden Ltd. in Baden, Switzerland, is a company that manufactures them for signals in the 75 Hz–30 MHz frequency range, and Flam and Russell, Inc. in Horsham, PA, makes them for the 2–30 MHz frequency band. Lincoln Lab at the Massachusetts Institute of Technology, Cambridge, has performed some preliminary localization tests with the EM vector sensors manufactured by Flam and Russell, Inc. [17]. Some other recent research on sensor development is reported in [23] and [24].

DOA estimation with EM vector sensors has been of much interest lately. Since Nehorai and Paldi [1], [2] proposed the use of EM vector sensors for DOA estimation, there have been a few studies of uniqueness [3]–[6], [16]. Various DOA estimation algorithms have also been suggested in [7]–[14], which have indicated the superiority of EM vector sensors over scalar sensors. In particular, it was revealed in [4]–[6] that with just an EM vector sensor, the DOA's and polarizations of up to three signals can be uniquely determined (seven or more distributed scalar sensors would be needed for the same purpose [25]).

Beamforming with EM vector sensors, however, has received little attention despite their potential advantages. Here, we list several advantages. First, a single EM vector sensor can beamform in a three-dimensional (3-D) space while occupying very little space. In contrast, conventional scalar-sensor methods require a two-dimensional (2-D) array to implement 3-D beamforming. Second, the findings reported in [1] and [2] shed light on the ability of vector sensors to receive/reject signals based on both their polarizations and DOA's. Polarization properties provide a crucial criterion for distinguishing and isolating signals that may otherwise overlap in conventional scalar-sensor arrays. Third, based on the results reported in [4]–[6] and the fact that EM vector sensors search in both the polarization and DOA domains, EM vector sensors should be able to handle more signals in beamforming applications as compared with (the same number of) scalar sensors. Conventional scalar-sensor arrays suffer from localization ambiguities because only the DOA information is exploited for such arrays. Fourth, since the steering vector of a single EM vector sensor is independent of the signal's frequency, it can process wideband signals in the same way as narrowband signals. In contrast, since the steering vector of a scalar-sensor array is dependent of the signal's frequency, this requires much higher computational costs to process wideband signals. Fifth, unlike a scalar-sensor array, an EM vector sensor does not need synchronization among measurements in different components of the sensor since there is no time delay among measurements.

Manuscript received May 16, 1997; revised August 6, 1998. The work of A. Nehorai was supported by the Air Force Office of Scientific Research under Grant F49620-97-1-0481, the National Science Foundation under Grant MIP-9615590, and the Office of Naval Research under Grant N00014-96-1-1078. The associate editor coordinating the review of this paper and approving it for publication was Dr. Yingbo Hua.

A. Nehorai is with the Department of Electrical Engineering and Computer Science, University of Illinois at Chicago, Chicago, IL 60607-7053 USA.

K.-C. Ho is with the Centre for Signal Processing, Nanyang Technological University, School of Electrical and Electronic Engineering, Singapore, Republic of Singapore.

B. T. G. Tan is with the Faculty of Science, National University of Singapore, Singapore, Republic of Singapore.

Publisher Item Identifier S 1053-587X(99)01327-6.

In this paper, we investigate the performance of a minimum-noise-variance type beamformer [26] for the case of one EM vector sensor, restricting our investigation to scenarios where there exist one signal and one interference that are uncorrelated. Such a beamformer requires the knowledge of the DOA and polarization parameters of the signal and assumes that the signal, interference, and noise are mutually uncorrelated. The beamformer minimizes the output variance while maintaining the gain in the direction of the signal. This has the effect of preserving the signal while minimizing contributions to the output due to interference and noise arriving from directions other than the DOA of the signal. Two types of signals are considered: One carries a single message, and the other carries two independent messages simultaneously [1], [2]. We will call the former a single-message (SM) signal and the latter a dual-message (DM) signal. On the other hand, the interference under consideration takes the form of a partially polarized (PP) signal, which can be completely polarized (CP) at one extreme and unpolarized (UP) at the other. Note that SM signals are CP, whereas DM signals are PP or UP.

We first obtain explicit expressions for the signal to interference-plus-noise ratio (SINR) in terms of the parameters of the signal, interference, and noise for both SM signals and DM signals. Then, we discuss some physical implications associated with the SINR expressions. In particular, we deduce that for the two types of signals of interest, the SINR rises with an increase in the separation between the DOA's and/or the polarizations of the signal and the interference for all DOA's and polarizations (scalar-sensor arrays and a single tripole do not have such properties). Moreover, we identify a strategy for effectively suppressing an interference with an EM vector sensor. The SINR expression for the SM signal that we derive also provides a basis for generating a DM signal in which the two message signals have minimum interference effect on one another. The analyses concerning SM and DM signals are presented in Sections III and IV, respectively. In Section V, we present numerical examples that are in agreement with our analyses. Finally, in Section VI, we analyze the characteristics of the main-lobe and side-lobe of the beampattern of an EM vector sensor and compare them with other types of sensor arrays.

II. Problem Formulation and Preliminary Discussion

We first introduce the abbreviations and notations used in this paper.

A. Abbreviations and Notations

1) Abbreviations:

EM Electromagnetic.
SINR Signal-to-interference-plus-noise ratio.
DOA Direction-of-arrival.
DM Dual-message.
SM Single-message.
DOP Degree of polarization.
CP Completely polarized.
PP Partially polarized.
UP Unpolarized.
PD Polarization difference.
ULA Uniform linear array.
UCA Uniform circular array.

2) Notations:

$(.)^T$, $(.)^H$, *	Transpose, Hermitian, and complex conjugate.
$\mathbf{I}_n$	$n \times n$ identity matrix.
$\mathbf{y}_s(t)$, $\mathbf{y}_d(t)$	6×1 complex envelope (phasor) measurement (both electric and magnetic fields) received at an EM vector sensor at time t associated with SM signal or DM signal.
$\mathbf{y}_E(t)$	3×1 complex envelope (phasor) electric field measurement.
$\mathbf{y}_H(t)$	3×1 complex envelope (phasor) magnetic field measurement.
$\mathbf{e}_E(t)$, $\mathbf{e}_H(t)$	3×1 complex envelope (phasor) electric and magnetic noise.
$s_s(t)$	Complex envelope of an SM signal.
$s_{d,1}(t)$, $s_{d,2}(t)$	Complex envelopes of the first and second message signals of a DM signal.
$\mathbf{R}_s$, $\mathbf{R}_d$	Covariance matrices of $\mathbf{y}_s(t)$, $\mathbf{y}_d(t)$.
$\mathbf{R}_i$	Interference covariance matrix.
$\mathbf{w}$	Weight vector of the minimum-noise-variance beamformer.
ϕ, ψ	Azimuth and elevation associated with a DOA.
α, β	Orientation and ellipticity angles associated with the polarization of a CP signal.
$\boldsymbol{\theta}$	Vector denoting $[\phi, \psi, \alpha, \beta]^T$.
$\mathbf{a}(\boldsymbol{\theta})$	Steering vector of an EM vector sensor for a CP signal with $\boldsymbol{\theta}$.
$\mathbf{B}(\phi, \psi)$	Steering matrix of an EM vector sensor for a UP signal with DOA (ϕ, ψ).
$\mathbf{Q}(\alpha)$	Rotation matrix with angle α.
$\mathbf{h}(\beta)$	2×1 unit-norm vector representing ellipticity of a polarization.
$\sigma_{i,c}^2$, $\sigma_{i,u}^2$	Powers of the CP and UP components of an interference.
σ_s^2	Power of an SM signal.
$\sigma_{d,1}^2$, $\sigma_{d,2}^2$	Powers of the first and second message signals of a DM signal.
σ^2	Power of the electric/magnetic noise.
Δ_i^s	Difference between the polarizations of an SM signal and interference.
$\Delta_i^{d,1}$	Difference between the polarizations of the first message signal (of a DM signal) and interference.
$\Delta_i^{d,2}$	Difference between the polarizations of the second message signal (of a DM signal) and interference.
γ	Angular separation between the DOA's of the signal and interference.
λ	Wavelength.

Note that we use the subscripts "s," "d," "d, 1," "d, 2," and "i" to associate some symbols with, respectively, the SM signal, the DM signal, the first and second messages of a

DM signal, and interference. For example, the symbols β_s, $\beta_{d,1}$, $\beta_{d,2}$, and β_i denote the ellipticity angles associated with, respectively, SM signal, the first and second messages of a DM signal, and interference.

Now, we shall describe the data models as proposed in [1] and [2] for an SM signal and a DM signal in Sections II-B and C, respectively.

B. Single-Message Signal

With the above notation, we have

$$\begin{aligned}\mathbf{y}_s(t) &\triangleq \begin{pmatrix}\mathbf{y}_E(t)\\ \mathbf{y}_H(t)\end{pmatrix}\\ &= \mathbf{a}(\boldsymbol{\theta}_s)s_s(t) + \mathbf{B}(\phi_i,\,\psi_i)\boldsymbol{\xi}_i(t) + \mathbf{e}(t)\end{aligned} \tag{2.1}$$

where

$$\begin{aligned}\mathbf{a}(\boldsymbol{\theta}) &= \mathbf{B}(\phi,\,\psi)\mathbf{Q}(\alpha)\mathbf{h}(\beta)\\ \boldsymbol{\theta} &= [\phi,\,\psi,\,\alpha,\,\beta]^T\\ \mathbf{B}(\phi,\,\psi) &= \begin{pmatrix}\mathbf{v}(\phi,\,\psi) & \tilde{\mathbf{v}}(\phi,\,\psi)\\ \tilde{\mathbf{v}}(\phi,\,\psi) & -\mathbf{v}(\phi,\,\psi)\end{pmatrix}\\ (\mathbf{v}(\phi,\,\psi)\quad \tilde{\mathbf{v}}(\phi,\,\psi)) &= \begin{pmatrix}-\sin\phi & -\cos\phi\sin\psi\\ \cos\phi & -\sin\phi\sin\psi\\ 0 & \cos\psi\end{pmatrix}\\ \mathbf{Q}(\alpha) &= \begin{pmatrix}\cos\alpha & \sin\alpha\\ -\sin\alpha & \cos\alpha\end{pmatrix}\\ \mathbf{h}(\beta) &= \begin{pmatrix}\cos\beta\\ j\sin\beta\end{pmatrix}\end{aligned} \tag{2.2}$$

$\mathbf{e}(t) = [\mathbf{e}_E^T(t), \mathbf{e}_H^T(t)]^T$, $s_s(t) \in \mathbb{C}^1$, $\boldsymbol{\xi}_i(t) \in \mathbb{C}^{2\times 1}$, $\mathbf{y}_E(t)$, $\mathbf{y}_H(t)$, $\mathbf{e}_E(t)$, $\mathbf{e}_H(t) \in \mathbb{C}^{3\times 1}$. The first, second, and third terms on the right-hand side of (2.1) correspond to measurements induced by, respectively, the signal, interference, and noise. Physically, $\mathbf{y}_E(t)$ and $\mathbf{y}_H(t)$ are, respectively, the three-component measurements of the electric and magnetic fields at the sensor at time t, and $\mathbf{e}_E(t)$ and $\mathbf{e}_H(t)$ are the noise components in these measurements. The parameters $\phi \in (-\pi,\,\pi]$ and $\psi \in [-\pi/2,\,\pi/2]$ are the azimuth and elevation of the signal, and $\alpha \in (-\pi/2,\,\pi/2]$ and $\beta \in [-\pi/4,\,\pi/4]$ are the polarization parameters, which are referred to as the orientation angle and ellipticity, respectively. The vector $\mathbf{a}(\boldsymbol{\theta})$ is the steering vector of an EM vector sensor associated with an SM signal with parameter $\boldsymbol{\theta}$, and $\mathbf{v}(\phi,\,\psi)$ and $\tilde{\mathbf{v}}(\phi,\,\psi)$ are unit vectors that span the same plane as the electric and magnetic field vectors of the incoming signal with DOA $(\phi,\,\psi)$. The variable $s_s(t)$ is the complex envelope of the signal and $\boldsymbol{\xi}_i(t)$ the complex envelopes of the interference.

The covariance of $\boldsymbol{\xi}_i(t)$ determines the state of polarization of the interference. Indeed, the interference covariance matrix $\mathbf{R}_i \triangleq E(\boldsymbol{\xi}_i(t)\boldsymbol{\xi}_i^H(t))$ can be expressed as (see [15, Lemma 1])

$$\mathbf{R}_i = \frac{\sigma_{i,u}^2}{2}\,\mathbf{I}_2 + \sigma_{i,c}^2\mathbf{Q}(\alpha_i)\mathbf{h}(\beta_i)\mathbf{h}^H(\beta_i)\mathbf{Q}^H(\alpha_i). \tag{2.3}$$

The first term on the right-hand side of (2.3) is the UP component with power $\sigma_{i,u}^2$, and the second is the CP component with power $\sigma_{i,c}^2$. The degree of polarization (DOP) of the interference is defined as the ratio between the power of the CP component and the total power of the interference, i.e., $\sigma_{i,c}^2/(\sigma_{i,u}^2+\sigma_{i,c}^2)$. The interference is said to be CP if $\sigma_{i,c}^2 \neq 0$ but $\sigma_{i,u}^2 = 0$, PP if $\sigma_{i,c}^2 \neq 0$ and $\sigma_{i,u}^2 \neq 0$, and UP if $\sigma_{i,u}^2 \neq 0$ but $\sigma_{i,c}^2 = 0$.

The output of a beamformer in this case is

$$\hat{s}_s(t) = \mathbf{w}_s^H\mathbf{y}_s(t) \tag{2.4}$$

where $\mathbf{w}_s \in \mathbb{C}^{6\times 1}$ is a weight vector. Suppose the DOA and polarization parameters of the signal are known; then, for the minimum-noise-variance beamformer, the weight vector is obtained through the constrained minimization

$$\mathbf{w}_s = \arg\min_{\mathbf{w}\in\mathbb{C}^{6\times 1}} \mathbf{w}^H\mathbf{R}_s\mathbf{w}, \qquad \text{subject to } \mathbf{w}^H\mathbf{a}_s = 1 \tag{2.5}$$

where $\mathbf{R}_s = E(\mathbf{y}_s(t)\mathbf{y}_s^H(t))$ is the data covariance matrix, and $\mathbf{a}_s$ denotes $\mathbf{a}(\boldsymbol{\theta}_s)$. The beamformer attempts to suppress all incoming interference except for the desired signal with steering vector $\mathbf{a}_s$.

C. Dual-Message Signal

The complex (phasor) sensor measurement obtained by an EM vector sensor at time t induced by a DM signal in the presence of an interference and additive noise is given by

$$\begin{aligned}\mathbf{y}_d(t) &= \mathbf{a}(\boldsymbol{\theta}_{d,1})s_{d,1}(t) + \mathbf{a}(\boldsymbol{\theta}_{d,2})s_{d,2}(t)\\ &\quad + \mathbf{B}(\phi_i,\,\psi_i)\boldsymbol{\xi}_i(t) + \mathbf{e}(t)\end{aligned} \tag{2.6}$$

where

$$\boldsymbol{\theta}_{d,1} = (\phi_d,\,\psi_d,\,\alpha_{d,1},\,\beta_{d,1})$$

and

$$\boldsymbol{\theta}_{d,2} = (\phi_d,\,\psi_d,\,\alpha_{d,2},\,\beta_{d,2}).$$

The first and second terms on the right-hand side of (2.6) correspond to measurements induced by, respectively, the first and second message signals associated with the DM signal, whereas the third and fourth terms correspond to the interference and noise, respectively. The variables $s_{d,k}(t)$ and $\mathbf{a}(\boldsymbol{\theta}_{d,k})$, where $k = 1, 2$, are the complex envelope and steering vector of the kth message signal. Note that the two steering vectors $\mathbf{a}(\boldsymbol{\theta}_{d,1})$ and $\mathbf{a}(\boldsymbol{\theta}_{d,2})$ have the same DOA $(\phi_d,\,\psi_d)$ but different polarizations $(\alpha_{d,1},\,\beta_{d,1}) \neq (\alpha_{d,2},\,\beta_{d,2})$. We will propose in Section IV an appropriate choice of $(\alpha_{d,1},\,\beta_{d,1})$ and $(\alpha_{d,2},\,\beta_{d,2})$ that minimizes the interference effect on one message signal due to the other.

The outputs of a beamformer for the first and second message signals are

$$\hat{s}_{d,1}(t) = \mathbf{w}_{d,1}^H\mathbf{y}_d(t) \quad \text{and} \quad \hat{s}_{d,2}(t) = \mathbf{w}_{d,2}^H\mathbf{y}_d(t)$$

where $\mathbf{w}_{d,1}$, $\mathbf{w}_{d,2} \in \mathbb{C}^{6\times 1}$ are the corresponding weight vectors. Note that in order to optimize the recovery of the message signals, a specific weight vector is used for each message signal separately. Suppose the DOA and polarization parameters of the signal are known. Then, for the minimum-noise-variance beamformer, the weight vector for the kth message signal, where $k = 1, 2$, is obtained through the constrained minimization

$$\mathbf{w}_{d,k} = \arg\min_{\mathbf{w}\in\mathbb{C}^{6\times 1}} \mathbf{w}^H\mathbf{R}_d\mathbf{w}, \quad \text{subject to } \mathbf{w}^H\mathbf{a}_{d,k} = 1 \tag{2.7}$$

where $\mathbf{R}_d = E(\mathbf{y}_d(t)\mathbf{y}_d^H(t))$ is the data covariance matrix, and $\mathbf{a}_{d,k}$ denotes $\mathbf{a}(\boldsymbol{\theta}_{d,k})$.

D. Assumptions

The analyzes to be carried out are based on the following.

Assumption 1: The DOA and polarization parameters of the signal are known.

Assumption 2: The complex envelopes of $s_s(t)$, $s_{d,1}(t)$, and $s_{d,2}(t)$, and of each components of $\mathbf{e}_E(t)$ and $\mathbf{e}_H(t)$, are all zero-mean Gaussian random variables.

Assumption 3: The signal is uncorrelated with the interference.

Assumption 4: The various components of the noise are uncorrelated among themselves and uncorrelated with both the signal and interference.

Assumption 5: The powers of the electric noise and magnetic noise are all equal to σ^2 (i.e., the noise covariance matrix is equal to $\sigma^2\mathbf{I}_6$).

Under Assumptions 2–5, the data covariance matrix is

$$\mathbf{R}_s = \sigma_s^2\mathbf{a}_s\mathbf{a}_s^H + \mathbf{B}_i\mathbf{R}_i\mathbf{B}_i^H + \sigma^2\mathbf{I}_6$$

for the case of SM signal, where $\sigma_s^2 = E(s_s(t)s_s^*(t))$ is the power of the signal, and

$$\mathbf{R}_d = \sigma_{d,1}^2\mathbf{a}_{d,1}\mathbf{a}_{d,1}^H + \sigma_{d,2}^2\mathbf{a}_{d,2}\mathbf{a}_{d,2}^H + \mathbf{B}_i\mathbf{R}_i\mathbf{B}_i^H + \sigma^2\mathbf{I}_6$$

for the case of DM signal, where $\sigma_{d,k}^2 = E(s_{d,k}(t)s_{d,k}^*(t))$ is the power of the kth message signal, where $k = 1, 2$.

E. Performance Measures

To evaluate the beamformer performance, we focus on the ratio between the output power of the signal and output power of the interference and noise (SINR). The SINR measure has been used as a performance indicator for beamformers in many studies. In our case, for the SM signal, the SINR is given by

$$\text{SINR}_s \triangleq \frac{\sigma_s^2\mathbf{w}_s^H\mathbf{a}_s\mathbf{a}_s^H\mathbf{w}_s}{\mathbf{w}_s^H(\mathbf{R}_s - \sigma_s^2\mathbf{a}_s\mathbf{a}_s^H)\mathbf{w}_s}. \tag{2.8}$$

For the DM signal, the SINR for the kth message signal $\hat{s}_{d,k}(t)$ is

$$\text{SINR}_{d,k} \triangleq \frac{\sigma_{d,k}^2\mathbf{w}_{d,k}^H\mathbf{a}_{d,k}\mathbf{a}_{d,k}^H\mathbf{w}_{d,k}}{\mathbf{w}_{d,k}^H(\mathbf{R}_d - \sigma_{d,k}^2\mathbf{a}_{d,k}\mathbf{a}_{d,k}^H)\mathbf{w}_{d,k}} \tag{2.9}$$

where $k = 1, 2$.

In this work, we will obtain explicit expressions for SINR_s, $\text{SINR}_{d,1}$, and $\text{SINR}_{d,2}$, and investigate their characteristics in terms of the various parameters of the signal, interference, and noise.

To interpret the SINR expressions, we introduce a parameter that provides a measure for the difference between the polarizations of two signals using the Poincaré sphere polarization representation [27]. First, let $(\phi_1, \psi_1, \alpha_1, \beta_1)$, and $(\phi_2, \psi_2, \alpha_2, \beta_2)$ be the DOA's/polarizations of two signals. For the Poincaré sphere representation, we need to consider a new coordinate system, where the DOA's of the two signals both lie in the x–y plane (such a coordinate system can always be obtained with an appropriate coordinate rotation). In such a new coordinate system, the ellipticity angle β_k of the signal will remain unchanged. However, the orientation angle α_k will change, and we denote it by α_k'. According to the Poincaré sphere representation, a polarization (α_k', β_k) is represented by a point (referred to as Poincaré point for convenience) on a sphere whose center is at the origin and radius is 1. The position vector of that point is

$$\mathbf{p}_k = [\cos\alpha'\cos 2\beta, \sin\alpha'\cos 2\beta, \sin 2\beta]^T. \tag{2.10}$$

Such a representation has two desirable properties. First, for two polarizations with the same orientation angle (with respect to the new coordinate system), the larger the difference in their ellipticity angles, the larger the distance between two Poincaré points associated with the two polarizations. Second, for two polarizations with the same ellipticity angle (with respect to the new coordinate system), the larger the difference in their orientation angles,[1] the larger the distance between two Poincaré points associated with the two polarizations. Thus, it is meaningful to take the *difference between the polarizations of the two signals* to be Δ_2^1, the shorter arc length joining $\mathbf{p}_1$ and $\mathbf{p}_2$, where $\mathbf{p}_1$ and $\mathbf{p}_2$ are, respectively, the representations for the polarizations (α_1', β_1) and (α_2', β_2) on the Poincaré sphere.

Remarks:

i) To obtain the difference between the polarizations of two signals, there is a need to know the polarizations as well as the DOA's of these signals.

ii) It can be shown that the difference between the polarizations of two signals is independent of the coordinate system.

iii) When dealing with the difference between the polarizations of two signals, we are concerned with only the polarizations of the CP components of the signals.

iv) The range of Δ_2^1 is $[0, \pi]$ (see [27]).

v) The arc length Δ_2^1 is related to the orientation and ellipticity angles through Lemma 1.

Lemma 1—Compton [22]: Consider polarizations (α_1, β_1) and (α_2, β_2) associated with two signals. Let (α_1', β_1) and (α_2', β_2) be the polarizations in a coordinate system such that the DOA's of these signals both lie in the x–y plane. Then

$$\cos^2\left(\frac{\Delta_2^1}{2}\right) = |\mathbf{h}^H(\beta_2)\mathbf{Q}^H(\alpha_2')\mathbf{Q}(\alpha_1')\mathbf{h}(\beta_1)|^2. \tag{2.11}$$

F. A Useful Result

Under Assumptions 1–5, it can be shown that the weight vectors satisfying, respectively, (2.5) and (2.7) are

$$\mathbf{w}_s = \frac{\mathbf{R}_s^{-1}\mathbf{a}_s}{\mathbf{a}_s^H\mathbf{R}_s^{-1}\mathbf{a}_s}$$

and

$$\mathbf{w}_{d,k} = \frac{\mathbf{R}_d^{-1}\mathbf{a}_{d,k}}{\mathbf{a}_{d,k}^H\mathbf{R}_d^{-1}\mathbf{a}_{d,k}}, \qquad k = 1, 2. \tag{2.12}$$

Substituting (2.12) directly into the expressions for SINR given by (2.8) and (2.9), the DOA's and polarizations of the signal

[1] The increase in difference between the orientation angles is valid within a certain (useful) range of the orientation angles.

and interference, as well as the noise power, will be hidden in two matrices whose inverses need to be evaluated. For ease of interpreting the dependence of SINR on the signal, interference, and noise, we need the following result, which is useful for simplifying the analysis of SINR expressions.

Lemma 2—Cox [28]: Let $\mathbf{R} = \sigma_k^2 \mathbf{a}\mathbf{a}^H + \mathbf{G} \in \mathbb{C}^{6\times 6}$, and

$$\hat{\mathbf{w}} = \arg \min_{\mathbf{w}\in\mathbb{C}^{6\times 1}} \mathbf{w}^H \mathbf{R}\mathbf{w}, \qquad \text{subject to } \mathbf{w}^H\mathbf{a} = 1$$

where $\mathbf{a} \in \mathbb{C}^{6\times 1}$ is as defined in (2.2), and σ_k is a real constant. If $\mathbf{G}$ is nonsingular, then

$$\frac{\sigma_k^2 \hat{\mathbf{w}}^H \mathbf{a}\mathbf{a}^H \hat{\mathbf{w}}}{\hat{\mathbf{w}}^H \mathbf{G}\hat{\mathbf{w}}} = \sigma_k^2 \mathbf{a}^H \mathbf{G}^{-1}\mathbf{a}.$$

G. Coordinate Rotation

Clearly, the analysis of the SINR expressions can be simplified somewhat with Lemma 2. However, the SINR would be, in terms of the general expressions for $\mathbf{a}(\boldsymbol{\theta})$, the steering vector of an EM vector sensor, which is very complex:

$$\mathbf{a}(\boldsymbol{\theta}) = \begin{pmatrix} -(\mathrm{c}_\alpha \mathrm{c}_\beta + j\,\mathrm{s}_\alpha \mathrm{s}_\beta)\mathrm{s}_\phi + (\mathrm{s}_\alpha \mathrm{c}_\beta - j\,\mathrm{c}_\alpha \mathrm{s}_\beta)\mathrm{c}_\phi \mathrm{s}_\psi \\ (\mathrm{c}_\alpha \mathrm{c}_\beta + j\,\mathrm{s}_\alpha \mathrm{s}_\beta)\mathrm{c}_\phi + (\mathrm{s}_\alpha \mathrm{c}_\beta - j\,\mathrm{c}_\alpha \mathrm{s}_\beta)\mathrm{s}_\phi \mathrm{s}_\psi \\ (-\mathrm{s}_\alpha \mathrm{c}_\beta + j\,\mathrm{c}_\alpha \mathrm{s}_\beta)\mathrm{c}_\psi \\ -(\mathrm{s}_\alpha \mathrm{c}_\beta - j\,\mathrm{c}_\alpha \mathrm{s}_\beta)\mathrm{s}_\phi - (\mathrm{c}_\alpha \mathrm{c}_\beta + j\,\mathrm{s}_\alpha \mathrm{s}_\beta)\mathrm{c}_\phi \mathrm{s}_\psi \\ (\mathrm{s}_\alpha \mathrm{c}_\beta - j\,\mathrm{c}_\alpha \mathrm{s}_\beta)\mathrm{c}_\phi - (\mathrm{c}_\alpha \mathrm{c}_\beta + j\,\mathrm{s}_\alpha \mathrm{s}_\beta)\mathrm{s}_\phi \mathrm{s}_\psi \\ (\mathrm{c}_\alpha \mathrm{c}_\beta + j\,\mathrm{s}_\alpha \mathrm{s}_\beta)\mathrm{c}_\psi \end{pmatrix}$$

where s_α and c_α denote $\sin\alpha$ and $\cos\alpha$, etc. Our strategy is to apply a sequence of three appropriate rotations of the original coordinate system so that for any general scenario, we can work with a new coordinate system for which the DOA of the signal is parallel to the x axis and that of the interference is in the x–y plane. The three rotations to be effected are, successively, as follows:

1) a rotation of $\tan^{-1}\kappa$ about the x axis of the original coordinate system, where κ is given by $-[\sin\psi_s \cos(\phi_i - \phi_s)\cos\psi_i - \cos\psi_s \sin\psi_i]/[\sin(\phi_i - \phi_s)\cos\psi_i]$;
2) a rotation of ψ_s about the y axis of the coordinate system that has been rotated according to 1);
3) a rotation of ϕ_s about the z axis of the coordinate system that has been rotated according to (2).

It can be shown that with such a sequence of coordinate rotations, SINR_s, $\mathrm{SINR}_{d,1}$, and $\mathrm{SINR}_{d,2}$, as defined in (2.8) and (2.9), remain invariant. Moreover, the separation between the DOA's and difference between the polarizations of the signal and interference remain unchanged (the latter follows from the definition of the difference between two polarizations presented in Section II-E). Consequently, we shall assume hereafter that $(\phi_s, \psi_s) = (\phi_{d,1}, \psi_{d,1}) = (\phi_{d,2}, \psi_{d,2}) = (0, 0)$, and $\psi_i = 0$ (i.e., the DOA of the signal is parallel to the x axis and that of the interference is in the x–y plane), which leads to considerable simplification of the analyzes of SINR expressions. With such a setup, the separation between the DOA's of the signal and interference is simply ϕ_i. In addition, the difference between the polarizations of the signal and interference Δ_i^s satisfies $\cos^2(\Delta_i^s/2) = |\mathbf{h}^H(\beta_i)\mathbf{Q}^H(\alpha_i)\mathbf{Q}(\alpha_s)\mathbf{h}(\beta_s)|^2$.

III. SINR for Single-Message Signal

For convenience, we shall refer to the angular separation between the DOA's of the signal and interference as DOA separation and denote it by γ. Moreover, we shall refer to the difference between the polarizations of the signal and interference as polarization difference (PD). Theorem 1 below expresses the SINR_s explicitly in terms of the DOA separation, PD, and powers of the signal, interference, and noise.

Theorem 1: The expression of SINR_s, as given in (2.8), can be expressed as

$$\mathrm{SINR}_s = \sigma_s^2 \left[\frac{2}{\sigma^2} - \frac{(1+\cos\gamma)^2}{(\sigma^2 + \sigma_{i,u}^2)} \times \left(\frac{\sigma_{i,u}^2}{2\sigma^2} + \frac{\sigma_{i,c}^2 \cos^2 \dfrac{\Delta_i^s}{2}}{2\sigma_{i,c}^2 + \sigma^2 + \sigma_{i,u}^2} \right) \right]. \tag{3.1}$$

Proof: See Appendix A.

Remarks:

i) For UP interference, the PD Δ_i^s is undefined and can take any value within $[0, \pi]$. However, $\sigma_{i,c}^2 = 0$ in this case, and the last term of (3.1) is zero regardless of the value of Δ_i^s.
ii) To obtain (3.1), we need to evaluate analytically the inverse of a 6×6 matrix, which is nontrivial. However, using Lemma A.1 in Appendix A, we can avoid such computation.

Before we proceed, recall that σ_s^2, $\sigma_{i,u}^2 + \sigma_{i,c}^2$, and σ^2 are, respectively, the powers of the signal, the interference, and noise. In addition, $\sigma_{i,u}^2$ and $\sigma_{i,c}^2$ are the powers of the UP and CP components of the interference. The interference is CP if $\sigma_{i,u}^2 = 0$ and UP if $\sigma_{i,c}^2 = 0$. In addition, γ and Δ_i^s are, respectively, the DOA separation and PD.

Clearly, SINR_s increases with an increase in the signal's power σ_s^2 but decreases with an increase in the noise power σ^2 as well as the power of the CP (i.e., $\sigma_{i,c}^2$) or UP (i.e., $\sigma_{i,u}^2$) component of the interference. However, the dependencies of SINR_s on PD and DOA separation are nontrivial and are established in the following corollaries.

Corollary 1: If $\sigma_{i,c}^2 \neq 0$ and $\gamma \neq \pi$, then SINR_s is an increasing function of Δ_i^s.

Corollary 2: If $\sigma_{i,u}^2 \neq 0$ or $\Delta_i^s \neq \pi$, then SINR_s is an increasing function of γ.

Corollary 3: If $\sigma_{i,c}^2 = 0$, then SINR_s is independent of Δ_i^s.

Corollary 4: SINR_s attains the maximum value $\mathrm{SINR}_s^{\max} = 2\sigma_s^2/\sigma^2$ when either $\gamma = \pi$ or both $\Delta_i^s = \pi$ and $\sigma_{i,u}^2 = 0$ are true. Moreover, $\mathrm{SINR}_s^{\max}$ simply takes the value of SINR_s in the absence of interference.

Corollary 5: For given (fixed) σ_s^2, $\sigma_{i,u}^2 + \sigma_{i,c}^2$, σ^2, and γ, the minimum of SINR_s is attained when $\Delta_i^s = 0$ and $\sigma_{i,u}^2 = 0$.

Proof: See Appendix B.

Remarks:

i) Corollary 1 means that SINR_s generally increases with an increase in the PD Δ_i^s, except for two special cases: a) $\sigma_{i,c}^2 = 0$ or b) $\gamma = \pi$. Note that case a) corresponds to scenarios where the interference is UP and case b)

to scenarios where the DOA of the signal is exactly opposite from that of the interference. For case a), the interference has no CP component, and thus, the PD should not affect SINR_s (see Corollary 3). On the other hand, by Corollary 4, SINR_s for case b) always attains the maximum value $\text{SINR}_s^{\max}$, regardless of the other signal parameters.

ii) A special case of Corollary 1 is that even if the DOA's of the signal and interference are identical, we can still increase the value of SINR_s by increasing the PD Δ_i^s. This is a feature that scalar-sensor arrays lack. Indeed, for a scalar-sensor array, if the DOA of the interference is identical to that of the signal, interference suppression is impossible regardless of the PD, the number of sensors, and array aperture.

iii) Corollary 2 means that SINR_s generally increases with an increase in the DOA separation γ, except for the case where both $\sigma_{i,u}^2 = 0$ and $\Delta_i^s = \pi$ hold. For the case where $\sigma_{i,u}^2 = 0$ and $\Delta_i^s = \pi$, $\text{SINR}_s^{\max}$ can always be attained regardless of the other signal parameters (see Corollary 4). Note that $\sigma_{i,u}^2 = 0$ means that the interference is CP, and $\Delta_i^s = \pi$ means that the PD is the largest possible. For a coordinate system where the DOA's of the signal and interference both lie in the x–y plane, such a PD arises when the polarizations associated with the signal and interference satisfy $(\alpha_s, \beta_s) = (\alpha_i \pm \pi, -\beta_i)$. Physically, the two polarization ellipses associated with the polarizations (α_s, β_s) and (α_i, β_i) have the same shape but have their major axes orthogonal to each other, and at the same time, the directions of spin of the electric fields associated with the two polarizations are opposite.

iv) By Corollary 3, if the interference is UP, then it is not possible to increase the SINR_s by varying the polarization of the signal (α_s, β_s).

v) Corollary 4 means that SINR_s attains the largest possible value $\text{SINR}_s^{\max}$ when either the DOA's of the signal and interference are opposite or when the interference is CP with largest possible polarization difference π. In either case, $\text{SINR}_s^{\max}$ obtained is equivalent to the SINR_s when there is no interference regardless of the interference's power (i.e., the interference becomes completely ineffective).

vi) Corollary 5 means that for any given DOA separation, SINR_s attains its lowest value when the interference is CP with polarization difference equal to 0.

The fact that SINR_s increases with an increase in the DOA separation or PD for all DOA's and polarizations (see Corollaries 1 and 2) is an important feature associated with an EM vector sensor. Indeed, this feature is desirable as it is natural to expect a higher SINR with a larger DOA separation or PD. In contrast, for scalar-sensor arrays and a single tripole, SINR_s does not necessarily increase with an increase in the separation in DOA's or polarizations (we will elaborate the case of a tripole in Section III-B).

The above corollaries are potentially useful in some applications. For example, we can exploit the fact that SINR_s increases with an increase in the PD (Corollary 1) to effectively suppress an interference if the DOA and the CP component of the polarization of the interference are known. Indeed, for a fixed DOA separation γ, we can maximize SINR_s by transmitting the signal with polarization such that the PD is the largest possible, i.e., $\Delta_i^s = \pi$. This would lead to $\text{SINR}_s = \sigma_s^2[2 - (1 + \cos\gamma)^2\sigma_{i,u}^2/2(\sigma^2 + \sigma_{i,u}^2)]/\sigma^2$. Clearly, if the interference is CP (i.e., $\sigma_{i,u}^2 = 0$), then SINR_s attains $\text{SINR}_s^{\max} = 2\sigma_s^2/\sigma^2$, which is the value when there is no interference, regardless of the DOA separation and the interference's power.

A. Comparisons with Scalar-Sensor Arrays

Beamformers using scalar-sensor arrays have been addressed in the literature [18]. Here, we shall discuss some advantages of using an EM vector sensor as compared with scalar-sensor arrays for beamforming in 3-D space. First, for a scalar-sensor array, at least three sensors are needed to perform beamforming, which means that it will occupy a larger space than an EM vector sensor. Second, when the DOA of the interference is identical to that of the signal, interference suppression is impossible regardless of the number of scalar sensors and the array aperture. In contrast, a single vector sensor can suppress an interference if the difference between the polarizatons of the signal and interference is nonzero [see Remark ii) of the corollaries to Theorem 1]. Third, consider a signal and an interference with sufficiently large DOA separation. Then, to suppress the interference with arbitrary DOA, only one EM vector sensor is needed. However, for the case of scalar-sensor array, at least four appropriately spaced scalar sensors are needed. Indeed, to suppress an interference, the steering vector associated with the interference must be linearly independent on that associated with the signal. In this connection, it has been shown that to ensure every two steering vectors with distinct DOA's to be linearly independent, one EM vector sensor is sufficient [4], but at least four scalar sensors with intersensor spacings all less than half-wavelength are needed for the case of scalar-sensor array [29]. This is a result of the fact that an EM vector sensor searches in both the polarization and DOA domains, whereas the scalar-sensor array uses only time delay information. Fourth, the SINR for a vector sensor is isotropic, whereas for a scalar-sensor array, it very much depends on the array geometry and does not necessarily increase with an increase in the DOA separation.

B. Comparisons with a Single Tripole

The beamformer using a single tripole has been addressed by Compton [22]. In [22], Compton investigated the performance of a single tripole in suppressing a CP interference on receiving an SM signal. From the results of [22], we can deduce that unlike the case of an EM vector sensor, the SINR for a single tripole does not necessarily increase with an increase in the DOA separation or the PD. We shall use two examples to illustrate this property. First, consider a signal and an interference with DOA's lying in the x–y plane and vertically and linearly polarized. Then, the electric fields induced by the signal and interference are identical (except for

a scale constant), and thus, it is impossible to discriminate the signal and interference regardless of their DOA separation. Thus, the SINR remains unchanged (which is the smallest possible) regardless of the DOA separation. Next, consider a signal and an interference with opposite DOA's and both lying in the x–y plane, and suppose that both of them are circularly polarized. Then, the SINR when the signal and interference have the same spin (the PD is 0) is larger than when they have opposite spins (the PD is π). [This is because the electric fields induced at a tripole due to the signal and interference, with opposite DOA's, are identical (except for a scale constant) if their directions of spin are opposite but are distinct if their directions of spin are identical.] Consequently, the SINR does not necessarily increase with an increase in the PD.

Compton has also established that the SINR for a single tripole is the lowest [with SINR being equal to $\sigma_s^2/(\sigma^2+\sigma_{i,c}^2)$] if one of the following three conditions holds.

1) The interference has the same DOA and polarization as the signal.
2) The DOA of the signal is opposite from that of the interference, and the polarizations of the signal and interference satisfy $\alpha_s = -\alpha_i$ and $\beta_s = -\beta_i$.
3) The signal and interference are both linearly polarized, and their electric fields are parallel to each other (i.e., $\alpha_s = \alpha_i = \pi/2$ and $\beta_s = \beta_i = 0$ in our setup).

We now examine the above three conditions for an EM vector sensor (for scenarios where there exist a CP interference and an SM signal). The SINR_s for an EM vector sensor is lowest only if condition 1) is satisfied, and the lowest SINR_s equals $2\sigma_s^2/(\sigma^2+2\sigma_{i,c}^2)$, which is higher than the lowest SINR obtained with a single tripole. As for condition 2), Corollary 4 states that as long as the DOA of the signal is opposite from that of the interference, SINR_s for an EM vector sensor always attains the maximum value $\text{SINR}_s^{\max}$ regardless of the polarizations of the signal and interference. On the other hand, high SINR_s can be obtained for an EM vector sensor even when condition 3) is met. Indeed, when condition 3) is met, the DOA separation may range from 0 to π. By Corollary 2, SINR_s can be increased by increasing the DOA separation, and by Corollary 4, SINR_s attains the maximum value $\text{SINR}_s^{\max}$ when the DOA of the signal is opposite from that of the interference.

Thus, a single EM vector sensor generally outperforms a single tripole in suppressing a CP interference when receiving an SM signal.

IV. SINR for Dual-Message Signal

A DM signal consists of two SM signals (or CP signals) with the same DOA but different polarizations. The effective polarization of such a DM signal varies with time, and thus, the state of polarization of a DM signal can either be PP or UP. To transmit a DM signal (consisting of two uncorrelated message signals), it is desirable that the interference effect of one message signal on the other be minimal. Since the DOA parameters associated with the two message signals are identical, it is possible to exploit the difference only in the polarization parameters to reduce the interference effect. In this connection, Corollary 4 of Theorem 1 provides a good way for choosing the polarizations. Indeed, consider the scenario where there is no external interference, and view one message signal as the desired CP signal and the other message signal as a CP "interference." Then, by Corollary 4 of Theorem 1, both $\text{SINR}_{d,1}$ and $\text{SINR}_{d,2}$ attain their maximum values if the difference between the polarizations of the two message signals is equal to π (i.e., when extracting one message signal, there is theoretically no interference effect due to the other). Therefore, we shall assume hereafter, that the polarizations of the two message signals are chosen in such a way that the PD is π, meaning that the polarizations satisfy $(\alpha_{d,1}, \beta_{d,1}) = (\alpha_{d,2} \pm \pi, -\beta_{d,2})$ [refer to Remark iii) of the corollaries to Theorem 1 for a relevant physical meaning].

For convenience, we will refer to the difference between the polarizations of the first message signal and the interference (i.e., $\Delta_i^{d,1}$) as the first PD and the difference between the polarizations of the second message signal and the interference (i.e., $\Delta_i^{d,2}$) as the second PD. Similar to the case of SM signal, we are able to express $\text{SINR}_{d,1}$ and $\text{SINR}_{d,2}$ explicitly in terms of the DOA separation, the first and the second PD's, and the powers of the two message signals, interference, and noise.

Theorem 2: If $(\alpha_{d,1}, \beta_{d,1}) = (\alpha_{d,2} \pm \pi, -\beta_{d,2})$, then

$$\begin{aligned}\text{SINR}_{d,1} &= \sigma_{d,1}^2\left[\frac{2}{\sigma^2} - \frac{(1+\cos\gamma)^2}{\sigma^4}\left(\mu + \nu\cos^2\frac{\Delta_i^{d,1}}{2} + \frac{\nu^2}{4\sigma^4\delta_1}(1+\cos\gamma)^2\sin^2\Delta_i^{d,1}\right)\right]\\ \text{SINR}_{d,2} &= \sigma_{d,2}^2\left[\frac{2}{\sigma^2} - \frac{(1+\cos\gamma)^2}{\sigma^4}\left(\mu + \nu\cos^2\frac{\Delta_i^{d,2}}{2} + \frac{\nu^2}{4\sigma^4\delta_2}(1+\cos\gamma)^2\sin^2\Delta_i^{d,2}\right)\right]\end{aligned} \tag{4.1}$$

where

$$\begin{aligned}\mu &= \frac{\sigma^2\sigma_{i,u}^2}{2(\sigma^2+\sigma_{i,u}^2)}\\ \nu &= \frac{\sigma^4\sigma_{i,c}^2}{(\sigma^2+\sigma_{i,u}^2)(2\sigma_{i,c}^2+\sigma^2+\sigma_{i,u}^2)}\end{aligned} \tag{4.2}$$

$$\begin{aligned}\delta_1 &= \frac{\sigma^2+2\sigma_{d,2}^2}{\sigma_{d,2}^2\sigma^2} - \frac{(1+\cos\gamma)^2}{\sigma^4}\left(\mu+\nu\sin^2\frac{\Delta_i^{d,1}}{2}\right)\\ \delta_2 &= \frac{\sigma^2+2\sigma_{d,1}^2}{\sigma_{d,1}^2\sigma^2} - \frac{(1+\cos\gamma)^2}{\sigma^4}\left(\mu+\nu\sin^2\frac{\Delta_i^{d,2}}{2}\right).\end{aligned} \tag{4.3}$$

Proof: See Appendix C.

Remarks:

i) Theorem 2 is derived based on the assumption that $\sigma_{d,1}^2$ and $\sigma_{d,2}^2$, which are the powers of the first and second message signals, respectively, are nonzero. If $\sigma_{d,1}^2$ or $\sigma_{d,2}^2$ is equal to zero, Theorem 2 reduces to the case of SM signals that have been addressed in Section III, and the derivation of the SINR expression is somewhat different from those of $\text{SINR}_{d,1}$ and $\text{SINR}_{d,2}$.

ii) To obtain the expressions of $\text{SINR}_{d,1}$ and $\text{SINR}_{d,2}$ in Theorem 2, there is a need to evaluate analytically the inverse of a 6×6 matrix, which is nontrivial. However, using Lemma A.1 in Appendix A, we are able to transform the problem to one involving inversion of matrices of dimensions 3×3 or lower.

Corollary 1: If $\sigma_{i,c}^2 \neq 0$ and $\gamma \neq \pi$, then $\text{SINR}_{d,k}$ is an increasing function of $\Delta_i^{d,k}$ for $k = 1, 2$.

Corollary 2: If $\sigma_{i,u}^2 \neq 0$ or $\Delta_i^{d,k} \neq \pi$, then $\text{SINR}_{d,k}$ is an increasing function of γ, for $k = 1, 2$.

Corollary 3: If $\sigma_{i,c}^2 = 0$, then $\text{SINR}_{d,k}$ is independent of $\Delta_i^{d,k}$ for $k = 1, 2$.

Corollary 4: $\text{SINR}_{d,k}$ attains the maximum value $\text{SINR}_{d,k}^{\max} = 2\sigma_{d,k}^2/\sigma^2$ when either $\gamma = \pi$ or both $\Delta_i^{d,k} = \pi$ and $\sigma_{i,u}^2 = 0$ are true for $k = 1, 2$. Moreover, $\text{SINR}_{d,k}^{\max}$ simply takes the value of $\text{SINR}_{d,k}$ in the absence of interference.

Corollary 5: For given (fixed) $\sigma_{d,1}^2$, $\sigma_{d,2}^2$, $\sigma_{i,u}^2 + \sigma_{i,c}^2$, σ^2, and γ, the minimum of $\text{SINR}_{d,k}$ is attained when $\Delta_i^{d,k} = 0$ and $\sigma_{i,u}^2 = 0$ for $k = 1, 2$.

Proof: See Appendix D.

Remarks:

i) The dependence of $\text{SINR}_{d,k}$ on $\Delta_i^{d,k}$, γ, $\sigma_{d,k}^2$, σ^2, $\sigma_{i,c}^2$, and $\sigma_{i,u}^2$, as presented in Corollaries 1–5 of Theorem 2, is basically identical to that of SINR_s on Δ_i^s, γ, σ_s^2, σ^2, $\sigma_{i,c}^2$, and $\sigma_{i,u}^2$, as presented in Corollaries 1–5 of Theorem 1. Therefore, the discussion concerning Corollaries 1–5 of Theorem 1 in Section III is applicable to Corollaries 1–5 of Theorem 2.

ii) Since $\mathbf{p}_{d,1}$ and $\mathbf{p}_{d,2}$, as defined in (2.10) [which correspond to the representation of, respectively, $(\alpha_{d,1}, \beta_{d,1})$ and $(\alpha_{d,2}, \beta_{d,2})$ on the Poincaré Sphere], are two antipodal points on the Poincaré sphere, it can be shown that the sum of the first PD $\Delta_i^{d,1}$,and the second PD $\Delta_i^{d,2}$ is equal to a constant π. Thus, an increase in the first PD will lead to a decrease in the second PD, and vice versa. This has two implications. First, by Corollary 1 of Theorem 2, increasing the value of the first (or second) PD will lead to an increase in $\text{SINR}_{d,1}$ (or $\text{SINR}_{d,2}$) but a decrease in $\text{SINR}_{d,2}$ (or $\text{SINR}_{d,1}$). Consequently, the values of both $\text{SINR}_{d,1}$ and $\text{SINR}_{d,2}$ cannot be increased simultaneously with a change in the polarization of the interference. Second, by Corollary 4 of Theorem 2, if the DOA separation is not equal to π, then $\text{SINR}_{d,1}$ attains its maximum value when the interference is CP and the first PD is equal to π. However, the second PD will become zero, and thus, by Corollary 5, $\text{SINR}_{d,2}$ attains its minimum value. Thus, for each DOA separation that is not equal to π, $\text{SINR}_{d,1}$ attains its maximum value if and only if $\text{SINR}_{d,2}$ attains its minimum value.

Since $\text{SINR}_{d,1}$ and $\text{SINR}_{d,2}$ are generally not identical, it is not easy to address the SINR for the DM signal as a whole. Here, we will consider the "worst" case and use $\text{SINR}_{\min} \triangleq \min\{\text{SINR}_{d,1}, \text{SINR}_{d,2}\}$, which gives the smaller value between $\text{SINR}_{d,1}$ and $\text{SINR}_{d,2}$ as a measure of the effective SINR. Next, we shall take the powers of the two message signals to be identical since it is reasonable to assume that both message signals are equally important. With these considerations, we can easily verify the following from Corollaries 1–3 of Theorem 2.

1) $\text{SINR}_{\min}$ increases with an increase in DOA separation.
2) $\text{SINR}_{\min}$ increases when the first (or the second) PD increases from 0 to $\pi/2$ but decreases when the first (or the second) PD increases from $\pi/2$ to π.
3) $\text{SINR}_{\min}$ is independent of the first and second PD's if the interference is UP.

There are no comparable results for scalar sensors simply because scalar sensors cannot receive two (independent) message signals simultaneously. On the other hand, the previous work [22] on the single tripole does not address the DM signal. Thus, we will not make comparisons with the scalar sensor or the tripole.

V. Numerical Results

In this section, we present some numerical examples we computed to assess the reliability of our theoretical prediction of the performance of an EM vector sensor as presented in Sections III and IV. First, exact data covariance matrices $\mathbf{R}_s$ and $\mathbf{R}_d$ were used in the experiments for checking the SINR expressions we derived. Next, to make our experiments realistic, we also generated $\mathbf{R}_s$ and $\mathbf{R}_d$ using a finite number of snapshots.

We simulated one SM signal and one interference impinging on an EM vector sensor. The signal was circularly polarized with positive spin (i.e., $\beta_s = \pi/4$). The signal, interference, and noise were uncorrelated, and the signal-to-noise ratio (SNR) and interference-to-noise ratio (INR) were both 10 dB. We first show the results for the case where infinitely many snapshots (i.e., exact $\mathbf{R}_s$ and $\mathbf{R}_d$) were used, and the SINR_s was computed based on the "raw" expression (without our simplifications) given by (2.8). Fig. 1(a) shows the values of SINR_s as a function of DOA separation when the DOP of the interference was 1 (i.e., $\sigma_{i,u}^2 = 0$, and hence, the interference was CP). The values of the PD considered were 0, $\pi/2$, and π, which correspond to interferences whose polarizations were, respectively, circular with positive spin (i.e., $\beta_i = \pi/4$), linear (i.e., $\beta_i = 0$), and circular with negative spin (i.e., $\beta_i = -\pi/4$). The scenarios in Fig. 1(b) and (c) were identical to those with Fig. 1(a), except that the DOP's of the interferences were, respectively, 0.5 (corresponding to PP interference with $\sigma_{i,c}^2 = \sigma_{i,u}^2$) and 0 (i.e., $\sigma_{i,c}^2 = 0$ and, hence, the interference was UP). The SINR_s in Fig. 1(a)–(c) confirm Corollaries 1–4 of Theorem 1, i.e., that SINR_s increases with an increase in the DOA separation or the PD, SINR_s is independent of the PD when the interference is UP [see Fig. 1(c)], and SINR_s attains the maximum value $2\sigma_s^2/\sigma^2$ when the DOA separation is π or when the interference is CP (DOP $= 1$) and the PD is π.

Next, we conducted a simulation for scenarios identical to those of Fig. 1(a)–(c) but with 200 snapshots, and the results are shown in Fig. 1(d)–(f) correspondingly. The data covariance matrix was computed using $\hat{\mathbf{R}}_s = \sum_{t=1}^{N} \mathbf{y}_s(t)\mathbf{y}_s^H(t)$,

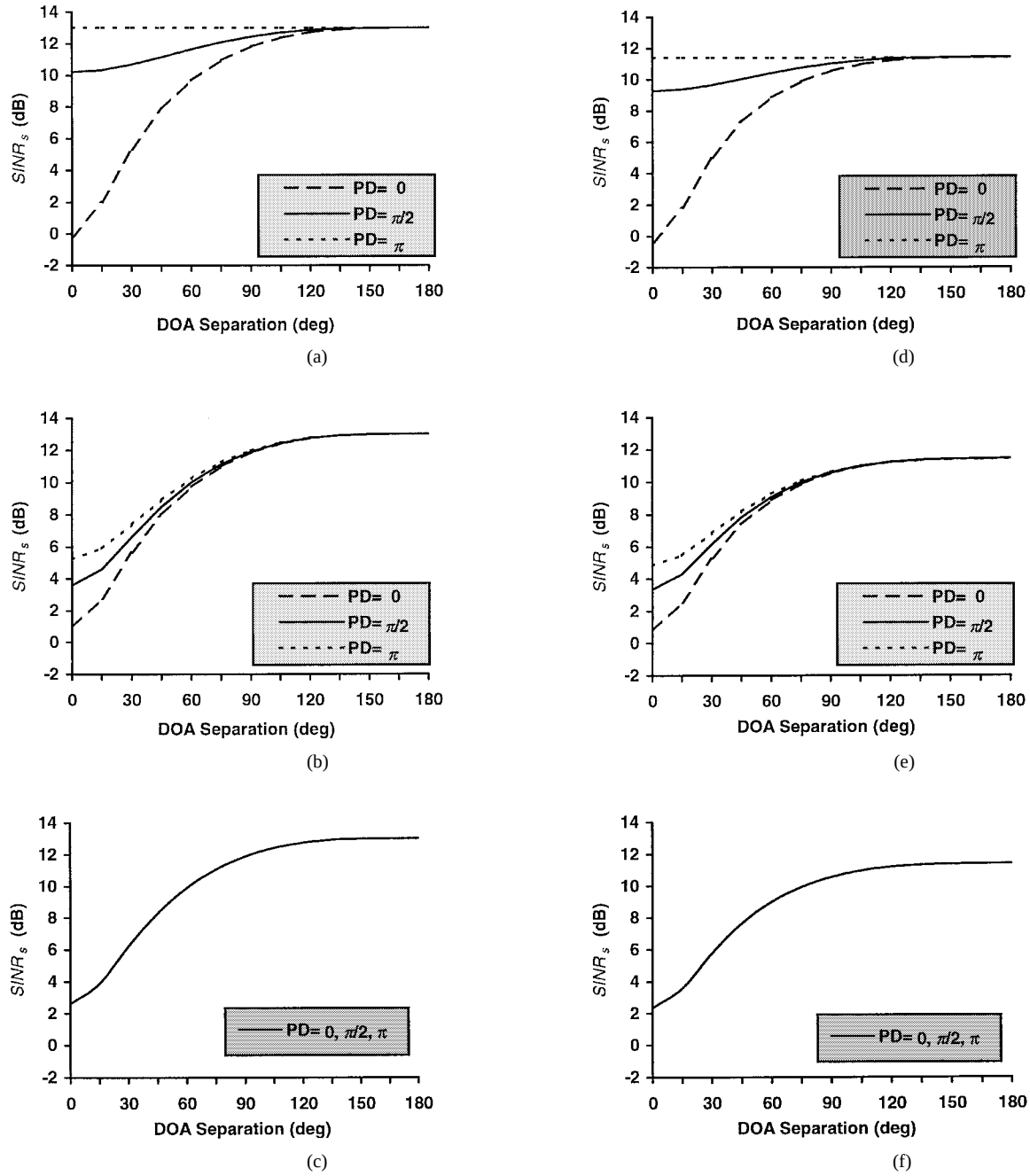

Fig. 1. (a) Graphs of SINR_s versus DOA separation for one SM signal and one interference uncorrelated with SNR = INR = 10 dB. The three curves correspond to PD $= 0$, PD $= \pi/2$, and PD $= \pi$. The DOP of the interference is 1, and true covariance is used. (b) As in (a), but the DOP of the interference is 0.5. (c) As in (a), but the DOP of the interference is 0. (d)–(f) As in (a)–(c), except that 200 snapshots are used. (a) DOP $= 1$; infinite snapshots available. (b) DOP $= 0.5$; infinite snapshots available. (c) DOP $= 0$; infinite snapshots available. (d) DOP $= 1$; 200 snapshots available. (e) DOP $= 0.5$; 200 snapshots available. (f) DOP $= 0$; 200 snapshots available.

where N is the number of snapshots, and SINR_s was computed as the average of the SINR_s's obtained based on 100 Monte Carlo runs. Comparing Fig. 1(d)–(f) with Fig. 1(a)–(c) correspondingly, we see that SINR_s obtained using 200 snapshots differs from that obtained using infinitely many snapshots by less than 2 dB. However, the dependencies of SINR_s on the various parameters are similar. Note that to achieve 10 dB SINR_s for all the above scenarios, the DOA separations have to be $\pi/3$ and $\pi/2$ or below for, respectively, the scenarios with infinitely many snapshots and those with finite snapshots.

We conducted simulations also for scenarios similar to those of Fig. 1(a)–(f) but with a DM signal, and the results were the same (see [30]).

VI. Beampattern of an Electromagnetic Vector Sensor

In this section, we first analyze the beampattern of an EM vector sensor and then make a comparison with two other types of sensor arrays. First, consider an EM vector sensor that has been steered toward (or focused in) the direction/polarization

$\boldsymbol{\theta}_F$ and assume that there is no noise and interference (an assumption adopted in some relevant studies such as [26] and [31]). Then, the normalized response (or beampattern) of the EM vector sensor due to an incident signal with direction/polarization $\boldsymbol{\theta}_k$ is given by

$$g(\boldsymbol{\theta}_F, \boldsymbol{\theta}_k) = |\mathbf{a}^H(\boldsymbol{\theta}_F)\mathbf{a}(\boldsymbol{\theta}_k)|^2/4. \tag{6.1}$$

[The function $g(\boldsymbol{\theta}_F, \boldsymbol{\theta}_k)$ reaches the maximum when $\boldsymbol{\theta}_k = \boldsymbol{\theta}_F$, and the maximum value attained is 1. Since the magnitude squared of $\mathbf{a}(\boldsymbol{\theta})$ is 4, we have introduced a denominator on the right-hand side of (6.1) so that the magnitude of $g(\boldsymbol{\theta}_F, \boldsymbol{\theta}_k)$ is normalized to 1 when $\boldsymbol{\theta}_k = \boldsymbol{\theta}_F$.] Note that unlike scalar-sensor arrays whose beampatterns are only functions of DOA, the beampattern of an EM vector sensor is dependent on both the DOA and polarization. To facilitate the analysis of the beampattern, we rotate the coordinate system (in the same way as that discussed in Section II-G) such that $\phi_F = \psi_F = \phi_k = 0$. Let the separation between the DOA's (ϕ_F, ψ_F) and (ϕ_k, ψ_k) be γ_k^F. Then, by Lemma A.3, (6.1) can be expressed as

$$g(\boldsymbol{\theta}_F, \boldsymbol{\theta}_k) = \frac{(1+\cos\gamma_k^F)^2}{4}\cos^2\frac{\Delta_k^F}{2} \tag{6.2}$$

where Δ_k^F is the difference between the polarization toward which the EM vector sensor is steered and the polarization of the incident signal. Although (6.2) is derived using the coordinate system where $\phi_F = \psi_F = \phi_k = 0$, it holds for any (ϕ_F, ψ_F) and (ϕ_k, ψ_k). This is because (6.2) is a function of only two parameters γ_k^F and Δ_k^F, which are both independent of the actual coordinate system.

From the expression of $g(\boldsymbol{\theta}_F, \boldsymbol{\theta}_k)$ given by (6.2), several properties of the beampattern of an EM vector sensor can be deduced. First, the response of an EM vector sensor in the direction/polarization $\boldsymbol{\theta}_k$ decreases with an increase in γ_k^F or Δ_k^F. Second, when $\gamma_k^F = \pi$ (i.e., at the direction opposite to the beam-steer direction) or when $\Delta_k^F = \pi$ (i.e., if the difference in polarizations is the largest possible), an EM vector sensor does not have any response. Finally, since $g(\boldsymbol{\theta}_F, \boldsymbol{\theta}_k)$ attains its maximum if and only if $\boldsymbol{\theta}_k = \boldsymbol{\theta}_F$, the beampattern of an EM vector sensor does not contain the grating lobe[2] (i.e., the side-lobe that is as high as the main-lobe). In contrast, the beampatterns for scalar sensors with uniform linear or uniform circular array geometry contain grating lobes (we will demonstrate this property in the latter part of this section), and such scalar sensors will not be able to suppress interferences arriving in the directions of the grating lobes.

Fig. 2 shows the polar plot of any cross-section of the beampattern that contains the beam-steer direction for $\Delta_k^F = 0,\ \pi/4,\ \pi/2,\ 3\pi/4$. Note that regardless of the beam-steer direction/polarization, the shape of the beampattern is identical to that shown in Fig. 2.

Now, we analyze the 3 dB (or half-power) beamwidth of the main-lobe. Since the beampattern of an EM vector sensor is dependent on polarization in addition to DOA, we will analyze the 3-dB beamwidth by considering a fixed value of Δ_k^F (as a result, the beampattern will depend only on the separation in DOA's). It can be deduced from (6.2) that for a fixed Δ_k^F, the 3-dB beamwidth is given by

$$\begin{cases} 2\cos^{-1}\left(\sqrt{2}/\cos\dfrac{\Delta_k^F}{2} - 1\right), & \text{if } \Delta_k^F \in [0, \pi/2] \\ 0, & \text{if } \Delta_k^F \in [\pi/2, \pi]. \end{cases}$$

In Fig. 3, we plot the 3-dB beamwidth as a function of Δ_k^F. This beamwidth decreases gradually from $13\pi/18$ to 0 if $\Delta_k^F \in [0, \pi/2]$. Beyond this interval (i.e., $\Delta_k^F \in [\pi/2, \pi]$), it is identically zero. This indicates the EM vector sensor's excellent ability in distinguishing signals and interferences that have sufficiently large differences in polarizations.

To further illustrate the performance of an EM vector sensor (as well as to facilitate comparisons with other types of sensor arrays to be discussed later), we show in Fig. 4(a) the beampattern when an EM vector sensor is steered toward the direction $(\phi_F, \psi_F) = (\pi/2, 0)$ and an arbitrary polarization with Δ_k^F being fixed at 0. For ease of visualizing the beampattern variation with respect to a reference fixed at -3 dB, we also show the horizontal plane cutting the z axis at -3

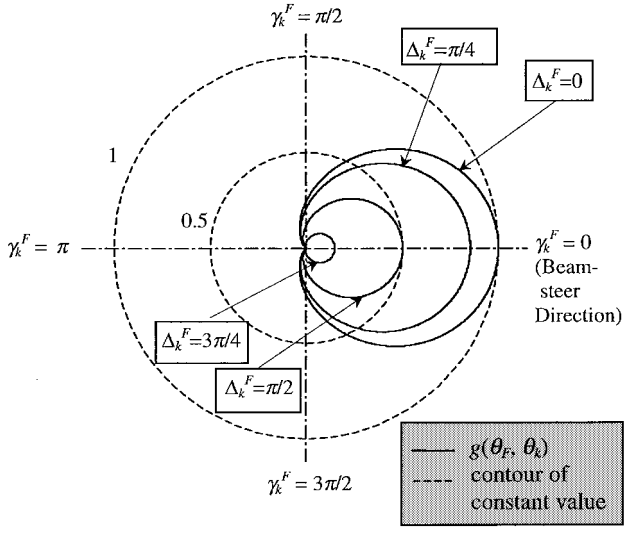

Fig. 2. Polar plot of a cross section of the beampattern of an EM vector sensor.

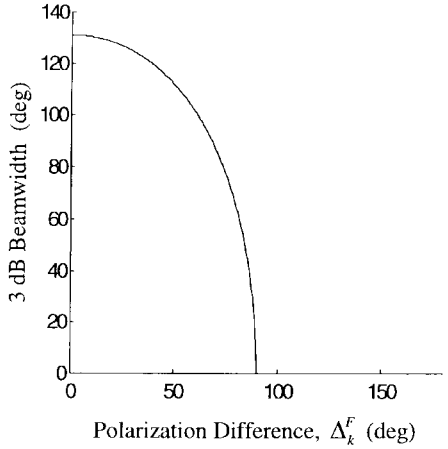

Fig. 3. Three-decibel beamwidth of an EM vector sensor against the polarization difference Δ_k^F.

[2] Such a property is also seen in the acoustic vector sensor, which measures the acoustic pressure and all the three components of the acoustic particle velocity induced by acoustic signals [32].

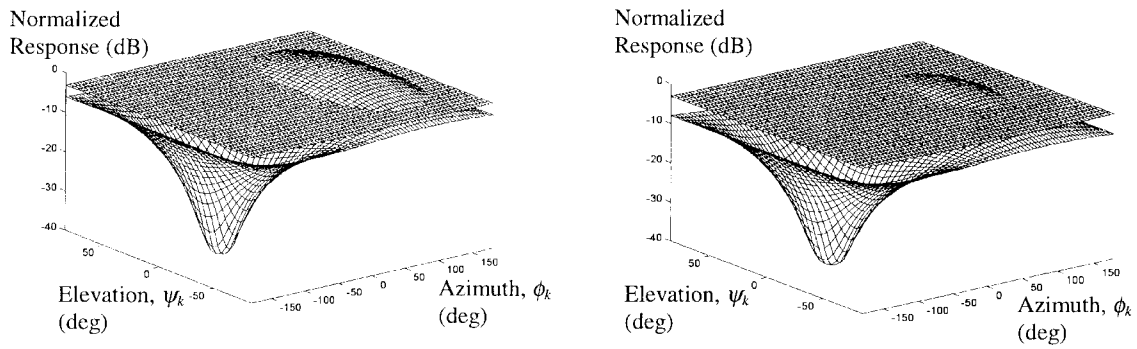

(a) (b)

Fig. 4. Beampatterns of an EM vector sensor with beam-steer directions $(\phi_F, \psi_F) = (\pi/2, 0)$. The values of Δ_k^F in (a) and (b) are, respectively, 0 and $7\pi/12$. The -3-dB plane is also shown.

dB. [Regardless of the beam-steer direction, the shape of the beampattern is identical to that shown in Fig. 4(a), except for a shift in position.] In Fig. 4(b), we show the beampattern for the case where the beam-steer direction is the same as that of Fig. 4(a) but with $\Delta_k^F = 7\pi/12$. [In Fig. 4(a) and (b), as well as the other figures to be presented subsequently, we truncate the value of the beampattern response to -40 dB if it is smaller or equal to -40 dB.]

We remark that since the beampattern of an EM vector sensor is dependent on both DOA and polarization, it is not obvious how to define a side-lobe for this sensor. However, for a fixed Δ_k^F, the beampattern is a decreasing function of γ_k^F [with maximum value at $(\phi_k, \psi_k) = (\phi_F, \psi_F)$]. Consequently, there is effectively no side-lobe for a fixed Δ_k^F.

We are now ready to compare the beampattern of an EM vector sensor with two types of sensors/arrays. We first consider arrays of six isotropic scalar sensors that measure only one component of the electric or magnetic field induced. Two common sensor configurations are considered: a six-sensor uniform linear array (ULA) lying along the y axis with intersensor spacing equal to $\lambda/2$, where λ is the wavelength of the signal of concern, and a six-sensor uniform circular array (UCA) with sensor coordinates $(\cos \pi\tau/3, \sin \pi\tau/3, 0)\lambda$ for $\tau = 0, \cdots, 5$. Note that unlike an EM vector sensor, the shapes of the beampatterns of the ULA and UCA are dependent on the beam-steer direction. Thus, to analyze the beampatterns, we have conducted simulations for many different beam-steer directions. An undesirable property of the beampatterns of the ULA and UCA is that they have grating-lobes. Moreover, many grating-lobes occur at directions that are very far from the beam-steer direction. For example, we plot in Figs. 5 and 6 the beampatterns of, respectively, the ULA and UCA, when the arrays are steered to $(\pi/2, 0)$, $(\pi/2, \pi/3)$, and $(\pi/2, \pi/2)$. In each figure, we also plot the -3 dB plane as in Fig. 4. For ULA, we see that the beampatterns contain many grating-lobes for all the beam-steer directions of concern. As for UCA, grating-lobes occur when the array is steered to $(\pi/2, \pi/3)$ and $(\pi/2, \pi/2)$, and a side-lobe with strength greater than -3 dB occurs when the array is steered to $(\pi/2, 0)$.

Next we consider an array consisting of two sets of sensors that are spatially displaced, one of which comprises three co-located orthogonal dipoles (called a tripole) and the other three co-located orthogonal loops (a dipole measures a component of the electric field induced by the signals, whereas a loop measures a component of the magnetic field). Such an array is similar to an EM vector sensor in the sense that both measure the complete components of electric and magnetic fields induced by EM signals. However, the three dipoles and three loops of such an array are spatially displaced, whereas those of an EM vector sensor are co-located. Due to the constraint on the paper length, we shall report only a brief analysis of some advantages and disadvantages of removing the spatial co-location characteristics of an EM vector sensor. The steering vector of the array at $\boldsymbol{\theta}$ (containing both DOA and polarization parameters) is $[\hat{\mathbf{a}}(\boldsymbol{\theta})^H, \tilde{\mathbf{a}}(\boldsymbol{\theta})^H]^H$, where $\hat{\mathbf{a}}(\boldsymbol{\theta}) = \hat{\mathbf{B}}(\phi, \psi)\mathbf{Q}(\alpha)\mathbf{h}(\beta)$ corresponds to the response of three co-located dipoles, $\tilde{\mathbf{a}}(\boldsymbol{\theta}) = d(\phi, \psi)\tilde{\mathbf{B}}(\phi, \psi)\mathbf{Q}(\alpha)\mathbf{h}(\beta)$ corresponds to that of three co-located loops, $\hat{\mathbf{B}}(\phi, \psi)$ and $\tilde{\mathbf{B}}(\phi, \psi)$ contain the first and the last three rows of $\mathbf{B}(\phi, \psi)$, respectively, and $d(\phi, \psi)$ is the phase delay between the two sensors due to a signal with DOA (ϕ, ψ). We will consider only the case where the coordinates of the sets of (co-located) dipoles and loops are (0, 0, 0) and (1, 0, 0)$\lambda/2$, respectively. An explicit analytical expression for the beampattern in terms of DOA and polarization is highly complex, and we will not attempt to pursue this direction. Instead, we will try to find out more about the characteristics of the beampattern by examining a large number of scenarios with different beam-steer directions/polarizations. In this connection, we discovered quite a number of scenarios where the beampatterns exhibit side-lobes having strength greater than -3 dB at directions that are very far from the beam-steer direction. Two such scenarios occur when the array is steered toward $\boldsymbol{\theta}_F = (\pi/2, 0, \pi/2, \pi/4)$ and $(\pi/4, 0, \pi/2, \pi/4)$ with the value of (α_k, β_k) fixed at $(\pi/2, -\pi/4)$ (the value of Δ_k^F for both scenarios is equal to π, which is the largest possible), and the beampatterns are plotted in Fig. 7(a) and (b), respectively. For Fig. 7(a), there are two side-lobes at $(\phi_F, \psi_F) = [-(7/9)\pi, 0]$ and $[-(2/9)\pi, 0]$, and for Fig. 7(b), there is one at $(\phi_F, \psi_F) = [-(11/18)\pi, 0]$. On the other hand, there are many scenarios where such an array outperforms an EM vector sensor because of better angular resolvability. This is due to the fact that such an array has a larger array aperture than an

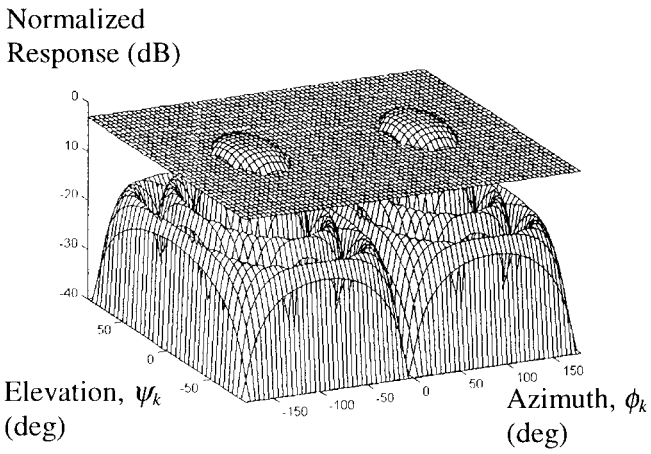

(a)

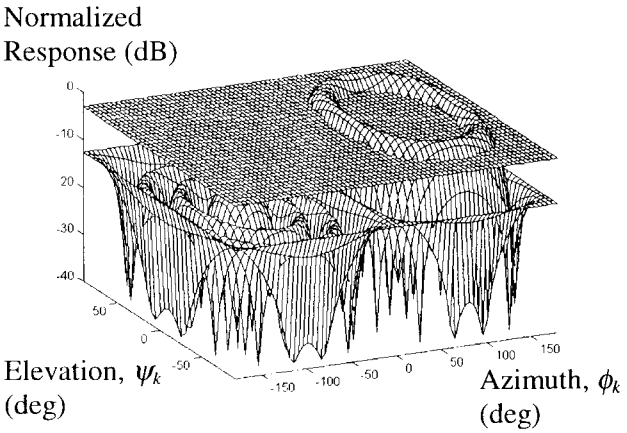

(b)

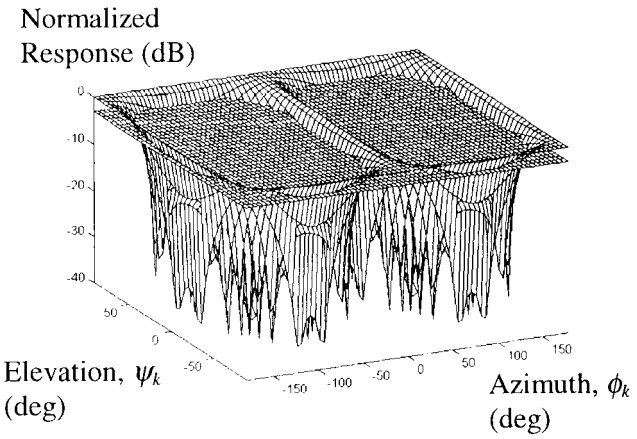

(c)

Fig. 5. (a)–(c) Beampatterns of a six-scalar sensor ULA lying along the y axis with intersensor spacing equal to half-wavelength. The beam-steer directions (ϕ_F, ψ_F) in (a)–(c) are, respectively, $(\pi/2, 0)$, $(\pi/2, \pi/3)$, and $(\pi/2, \pi/2)$. The -3-dB horizontal plane is also shown in each figure.

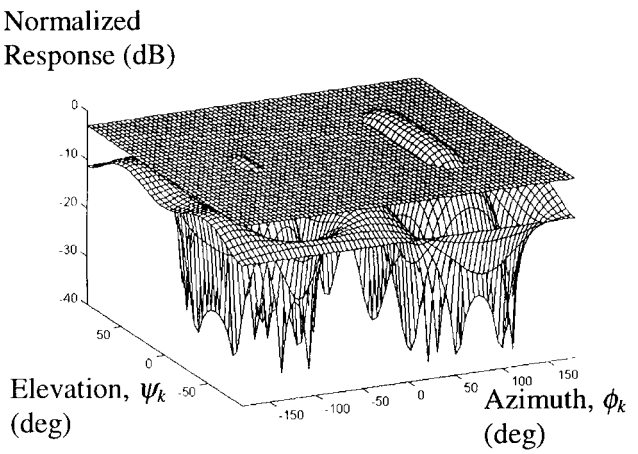

(a)

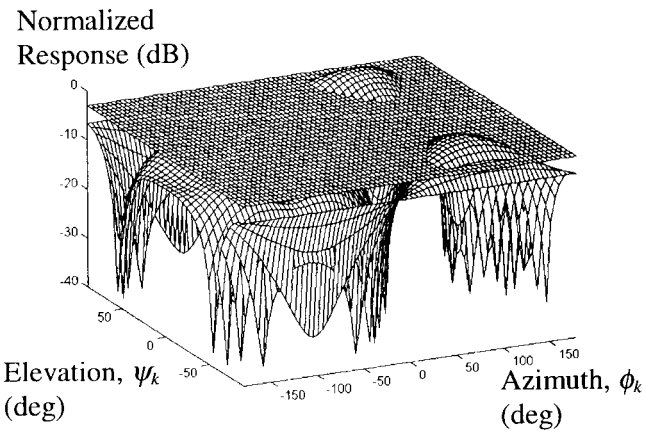

(b)

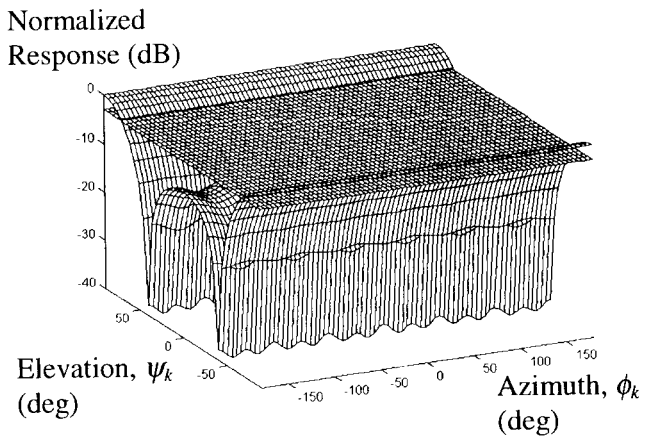

(c)

Fig. 6. (a)–(c) Same as Fig. 5(a)–(c), except that the array is a six-scalar sensor UCA with sensor coordinates $(\cos \pi\tau/3,\ \sin \pi\tau/3, 0)\lambda$, for $\tau = 0, \cdots, 5$.

EM vector sensor. Of course, the associated shortcoming is that it occupies a larger space physically.

VII. Conclusion

We have developed a minimum-noise-variance type beamformer employing an EM vector sensor for one signal and one interference that are uncorrelated. Both single-message and dual-message signals were considered, and the state of polarization of the interference under consideration ranged from completely polarized to unpolarized. To analyze the beamformer performance, we first obtained an explicit expression for the SINR of a single-message signal in terms of the parameters of the signal, interference, and noise. We deduced that the SINR of single-message signal increases with an increase in the separation between the DOA's and/or

the polarizations for all DOA's and polarizations (scalar-sensor arrays and a single tripole [22] do not have such properties). We also deduced that a single EM vector sensor can suppress an (uncorrelated) interference that has the same DOA as the signal and distinct polarizations (this is impossible for scalar sensors regardless of the number of sensors and the array aperture). In addition, we identified a strategy for effectively suppressing the interference, and through the SINR expression we derived, we also provided a basis for generating dual-message signals of which the two message signals have minimum interference effect on one another.

We derived an explicit expression for the SINR of such a dual-message signal in terms of the parameters of the signal, interference, and noise. Subsequently, we deduced that the above-mentioned characteristics for the SINR of a single-message signal were also valid for the SINR of a dual-message signal. We conducted fairly extensive computer simulations, and the results obtained were in good agreement with those of our analysis. Finally, we have also analyzed the characteristics of the main-lobe and side-lobe of the beampattern of an EM vector sensor and demonstrated the advantage of an EM vector sensor over some scalar-sensor arrays. In particular, we have shown that the beampattern of an EM vector sensor does not contain grating-lobes. In contrast, the beampatterns of a six-sensor uniform linear array and a six-sensor uniform circular array have grating-lobes. Moreover, many grating-lobes occur at directions that are very far from the beam-steer direction. A comparison of the beamforming performance of an EM vector sensor and an array of one electric and one magnetic vector sensors being separated at half-wavelength distance was also presented.

Our proposed beamformer can be extended easily to handle multiple sources with diverse polarizations using multiple vector sensors as receivers. Some possible follow-up studies are

i) investigation of the beamforming performance of an EM vector sensor for multiple signals and multiple interferences;
ii) performance with multiple EM vector sensors;
iii) performance for the signal and interference that are correlated;
iv) performance when the powers of the electric noise and magnetic noise at EM vector sensors are not identical;
v) effects of channel depolarization on the signal;
vi) comparison of an EM vector sensor with other types of EM sensors.

APPENDIX A
PROOF OF THEOREM 1

We first state a lemma and then establish two lemmas.

Lemma A.1—Golub and Van Loan [33]: Let $\mathbf{W} \in \mathbb{C}^{k\times k}$ and $\mathbf{X}, \mathbf{Y} \in \mathbb{C}^{k\times l}$, and suppose $\mathbf{W}$ and $(\mathbf{I}_l + \mathbf{Y}^H\mathbf{W}^{-1}\mathbf{X})$ are invertible. Then

$$(\mathbf{W}+\mathbf{X}\mathbf{Y}^H)^{-1} = \mathbf{W}^{-1} - \mathbf{W}^{-1}\mathbf{X}(\mathbf{I}_l + \mathbf{Y}^H\mathbf{W}^{-1}\mathbf{X})^{-1}\mathbf{Y}^H\mathbf{W}^{-1}.$$

Lemma A.2: Suppose $\mathbf{R}_i$ as defined in (2.3) is invertible. Then

$$\left(\mathbf{R}_i^{-1} + \frac{2}{\sigma^2}\mathbf{I}_2\right)^{-1} = \mu\mathbf{I}_2 + \nu\mathbf{q}_i\mathbf{q}_i^H$$

where $\mathbf{q}_i = \mathbf{Q}(\alpha_i)\mathbf{h}(\beta_i)$, and $\mathbf{Q}$ and $\mathbf{h}$ are as defined in (2.2) and μ and ν in (4.2).

Proof of Lemma A.2: Using Lemma A.1 with $\mathbf{W} = (2/\sigma^2)\mathbf{I}_2$, $\mathbf{X} = \mathbf{R}_i^{-1}$ and $\mathbf{Y}^H = \mathbf{I}_2$, we obtain

$$\begin{aligned}\left(\mathbf{R}_i + \frac{2}{\sigma^2}\mathbf{I}_2\right)^{-1} &= \frac{\sigma^2}{2}\mathbf{I}_2 - \frac{\sigma^4}{4}\mathbf{R}_i^{-1}\left(\mathbf{I}_2 + \frac{\sigma^2}{2}\mathbf{R}_i^{-1}\right)^{-1} \\ &= \frac{\sigma^2}{2}\mathbf{I}_2 - \frac{\sigma^4}{4}\left(\mathbf{R}_i + \frac{\sigma^2}{2}\mathbf{I}_2\right)^{-1}.\end{aligned}$$

Substituting the expression of $\mathbf{R}_i$ as given in (2.3) into the right-hand side of the above equation, we have

$$\begin{aligned}&\left(\mathbf{R}_i^{-1} + \frac{2}{\sigma^2}\mathbf{I}_2\right)^{-1} \\ &\quad= \frac{\sigma^2}{2}\mathbf{I}_2 - \frac{\sigma^4}{4}\left(\frac{\sigma^2+\sigma_{i,u}^2}{2}\mathbf{I}_2 + \sigma_{i,c}^2\mathbf{q}_i\mathbf{q}_i^H\right)^{-1}.\end{aligned}$$

Now, using Lemma A.1 with $\mathbf{W} = ((\sigma^2+\sigma_{i,u}^2)/2)\mathbf{I}_2$ and $\mathbf{X} = \mathbf{Y} = \sigma_{i,c}\mathbf{q}_i$, we get (after some manipulation)

$$\left(\mathbf{R}_i^{-1} + \frac{2}{\sigma^2}\mathbf{I}_2\right)^{-1} = \mu\mathbf{I}_2 + \nu\mathbf{q}_i\mathbf{q}_i^H. \qquad \blacksquare$$

Lemma A.3: Let $(\phi_1, \psi_1) = (0, 0)$ and $\psi_2 = 0$. Then

$$\|\mathbf{a}_1\mathbf{B}_2\|^2 = (1+\cos\phi_2)^2$$

and

$$|\mathbf{a}_1^H\mathbf{a}_2|^2 = (1+\cos\phi_2)^2\cos^2\frac{\Delta_2^1}{2}.$$

Proof of Lemma A.3: Since $(\phi_1, \psi_1) = (0, 0)$ and $\psi_2 = 0$, it can be verified that $\mathbf{B}_2^H\mathbf{B}_1 = (1+\cos\phi_2)\mathbf{I}_2$. Thus

$$\begin{aligned}\|\mathbf{a}_1^H\mathbf{B}_2\|^2 &= \mathbf{h}_1^H\mathbf{Q}_1^H(\mathbf{B}_1^H\mathbf{B}_2\mathbf{B}_2^H\mathbf{B}_1)\mathbf{Q}_1\mathbf{h}_1 \\ &= (1+\cos\phi_2)^2\mathbf{h}_1^H\mathbf{Q}_1^H\mathbf{Q}_1\mathbf{h}_1 \\ &= (1+\cos\phi_2)^2.\end{aligned}$$

Next, we have $|\mathbf{a}_1^H\mathbf{a}_2|^2 = |\mathbf{h}_1^H\mathbf{Q}_1^H(\mathbf{B}_1^H\mathbf{B}_2)\mathbf{Q}_2\mathbf{h}_2|^2 = (1+\cos\phi_2)^2|\mathbf{h}_1^H\mathbf{Q}_1^H\mathbf{Q}_2\mathbf{h}_2|^2$. By Lemma 1, we obtain $|\mathbf{h}_1^H\mathbf{Q}_1^H\mathbf{Q}_2\mathbf{h}_2|^2 = \cos^2(\Delta_2^1/2)$, and thus, the above equation reduces to

$$|\mathbf{a}_1^H\mathbf{a}_2|^2 = (1+\cos\phi_2)^2\cos^2\left(\frac{\Delta_2^1}{2}\right). \qquad \blacksquare$$

Proof of Theorem 1: We will consider two cases that cover all possible scenarios: a) $\sigma_{i,u}^2 = 0$ (i.e., the interference is CP) and b) $\sigma_{i,u}^2 \neq 0$ (i.e., the interference is PP or UP).

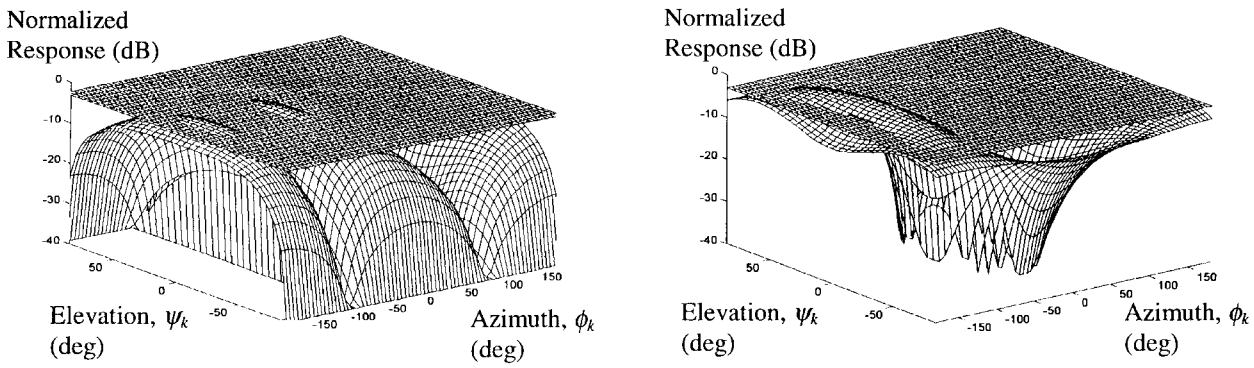

Fig. 7. (a) and (b) Beampatterns of two sets of sensors, one comprising three co-located dipoles and the other three co-located loops. These sensors lie along the x axis with intersensor spacing equal to half-wavelength. The beam-steer directions/polarizations in (a) and (b) are, respectively, $\boldsymbol{\theta}_F = (\pi/2,\ 0,\ \pi/2,\ \pi/4)$ and $\boldsymbol{\theta}_F = (\pi/4,\ 0,\ \pi/2,\ \pi/4)$, and $\Delta_k^F = \pi$.

Case a) $\sigma_{i,u}^2 = 0$*:* By Lemma 2, we can express the SINR$_s$ given in (2.8) as

$$\begin{aligned}\text{SINR}_s &= \sigma_s^2 \mathbf{a}_s^H (\mathbf{R}_s - \sigma_s^2 \mathbf{a}_s \mathbf{a}_s^H)^{-1} \mathbf{a}_s \\ &= \sigma_s^2 \mathbf{a}_s^H (\sigma_{i,c}^2 \mathbf{a}_i \mathbf{a}_i^H + \sigma^2 \mathbf{I}_6)^{-1} \mathbf{a}_s.\end{aligned}$$

Using Lemma A.1 with $\mathbf{W} = \sigma^2 \mathbf{I}_6$ and $\mathbf{X} = \mathbf{Y} = \sigma_{i,c} \mathbf{a}_i$, we obtain

$$\begin{aligned}\text{SINR}_s &= \sigma_s^2 \mathbf{a}_s^H \left(\frac{1}{\sigma^2} \mathbf{I}_6 - \frac{\sigma_{i,c}^2 \mathbf{a}_i \mathbf{a}_i^H}{\sigma^4 \left(1 + \dfrac{\sigma_{i,c}^2}{\sigma^2} \mathbf{a}_i^H \mathbf{a}_i \right)} \right) \mathbf{a}_s \\ &= \sigma_s^2 \left(\frac{2}{\sigma^2} - \frac{\sigma_{i,c}^2 |\mathbf{a}_s^H \mathbf{a}_i|^2}{\sigma^2 (\sigma^2 + 2\sigma_{i,c}^2)} \right).\end{aligned}$$

By Lemma A.3, $|\mathbf{a}_s^H \mathbf{a}_i|^2 = (1+\cos\gamma)^2 \cos^2(\Delta_i^s/2)$, and thus

$$\text{SINR}_s = \sigma_s^2 \left(\frac{2}{\sigma^2} - \frac{\sigma_{i,c}^2 (1+\cos\gamma)^2 \cos^2 \dfrac{\Delta_i^s}{2}}{\sigma^2 (\sigma^2 + 2\sigma_{i,c}^2)} \right) \qquad \text{(A.1)}$$

which is equal to the expression of SINR$_s$ given in Theorem 1 when $\sigma_{i,u}^2 = 0$.

Case b) $\sigma_{i,u}^2 \neq 0$*:* By Lemma 2, we can express SINR$_s$ given in (2.8) as

$$\begin{aligned}\text{SINR}_s &= \sigma_s^2 \mathbf{a}_s^H (\mathbf{R}_s - \sigma_s^2 \mathbf{a}_s \mathbf{a}_s^H)^{-1} \mathbf{a}_s \\ &= \sigma_s^2 \mathbf{a}_s^H (\mathbf{B}_i \mathbf{R}_i \mathbf{B}_i^H + \sigma^2 \mathbf{I}_6)^{-1} \mathbf{a}_s.\end{aligned}$$

Since $\sigma_{i,u}^2 \neq 0$, the matrix $\mathbf{R}_i$ is invertible. Now, using Lemma A.1 with $\mathbf{W} = \sigma^2 \mathbf{I}_6$, $\mathbf{X} = \mathbf{Y} = \mathbf{B}_i \mathbf{C}$, where $\mathbf{C}$ is a 2×2 matrix such that $\mathbf{C}\mathbf{C}^H = \mathbf{R}_i$, we get

$$\begin{aligned}\text{SINR}_s &= \sigma_s^2 \mathbf{a}_s^H \left(\frac{1}{\sigma^2} \mathbf{I}_6 - \frac{1}{\sigma^4} \mathbf{B}_i \mathbf{C} \left(\mathbf{I}_2 + \frac{1}{\sigma^2} \mathbf{C}^H \mathbf{B}_i^H \mathbf{B}_i \mathbf{C} \right)^{-1} \right. \\ &\qquad \left. \times \mathbf{C}^H \mathbf{B}_i^H \right) \mathbf{a}_s \\ &= \sigma_s^2 \mathbf{a}_s^H \left(\frac{1}{\sigma^2} \mathbf{I}_6 - \frac{1}{\sigma^4} \mathbf{B}_i \left(\mathbf{R}_i^{-1} + \frac{1}{\sigma^2} \mathbf{B}_i^H \mathbf{B}_i \right)^{-1} \right. \\ &\qquad \left. \times \mathbf{B}_i^H \right) \mathbf{a}_s \\ &= \sigma_s^2 \left(\frac{2}{\sigma^2} - \frac{1}{\sigma^4} \mathbf{a}_s^H \mathbf{B}_i \left(\mathbf{R}_i^{-1} + \frac{2}{\sigma^2} \mathbf{I}_2 \right)^{-1} \mathbf{B}_i^H \mathbf{a}_s \right).\end{aligned}$$

Now, substituting the inverse of $(\mathbf{R}_i^{-1} + (2/\sigma^2)\mathbf{I}_2)$ established in Lemma A.2 and after some manipulation, we have

$$\begin{aligned}\text{SINR}_s = \sigma_s^2 \left(\frac{2}{\sigma^2} - \frac{\sigma_{i,u}^2 \|\mathbf{a}_s^H \mathbf{B}_i\|^2}{2\sigma^2 (\sigma^2 + \sigma_{i,u}^2)} \right. \\ \left. - \frac{\sigma_{i,c}^2 |\mathbf{a}_s^H \mathbf{a}_i|^2}{(\sigma^2 + \sigma_{i,u}^2)(2\sigma_{i,c}^2 + \sigma^2 + \sigma_{i,u}^2)} \right).\end{aligned}$$

Since, by Lemma A.3, $\|\mathbf{a}_s^H \mathbf{B}_i\|^2 = (1+\cos\gamma)^2$ and $|\mathbf{a}_s^H \mathbf{a}_i|^2 = (1+\cos\gamma)^2 \cos^2(\Delta_i^s/2)$, we obtain

$$\begin{aligned}\text{SINR}_s = \sigma_s^2 \left(\frac{2}{\sigma^2} - \frac{\sigma_{i,u}^2 (1+\cos\gamma)^2}{2\sigma^2 (\sigma^2 + \sigma_{i,u}^2)} \right. \\ \left. - \frac{\sigma_{i,c}^2 (1+\cos\gamma)^2 \cos^2 \dfrac{\Delta_i^s}{2}}{(\sigma^2 + \sigma_{i,u}^2)(2\sigma_{i,c}^2 + \sigma^2 + \sigma_{i,u}^2)} \right). \qquad \text{(A.2)}\end{aligned}$$

Combining (A.1) for Case a) and (A.2) for Case b), we obtain Theorem 1. ■

APPENDIX B
PROOF OF COROLLARIES 1–5 OF THEOREM 1

Corollary 1 follows from the fact that $\cos^2(\Delta_i^s/2)$ is a decreasing function of Δ_i^s, and Corollary 2 follows from the

fact that $(1+\cos\gamma)^2$ is a decreasing function of γ. The proof of Corollary 3 is quite straightforward. Corollary 4 follows from the fact that $(1+\cos\gamma)^2$ and $\cos^2(\Delta_i^s/2)$ equals 0 at, respectively, $\gamma=\pi$ and $\Delta_i^s=\pi$.

Next, we shall establish Corollary 5. Consider a fixed DOA separation γ. Since σ_s^2, $\sigma_{i,u}^2+\sigma_{i,c}^2$, and σ^2 are fixed, the variables that affect SINR_s are $\sigma_{i,u}^2$ (or $\sigma_{i,c}^2$) and Δ_i^s. By Corollary 1 of Theorem 1, SINR_s for a given $\sigma_{i,u}^2$ will attain its minimum value

$$\begin{aligned}\text{SINR}_s^{\min}(\sigma_{i,u}^2)&=\sigma_s^2\left(\frac{2}{\sigma^2}-\frac{(1+\cos\gamma)^2}{(\sigma^2+\sigma_{i,u}^2)}\right.\\&\qquad\left.\times\left(\frac{\sigma_{i,u}^2}{2\sigma^2}+\frac{\sigma_{i,c}^2}{2\sigma_{i,c}^2+\sigma^2+\sigma_{i,u}^2}\right)\right)\\&=\sigma_s^2\left(\frac{2}{\sigma^2}-\frac{(1+\cos\gamma)^2(2\sigma_{i,c}^2+\sigma_{i,u}^2)}{2\sigma_{i,c}^2+\sigma^2+\sigma_{i,u}^2}\right)\end{aligned}\tag{B.1}$$

at $\Delta_i^s=0$. Now, it remains to be shown that $\text{SINR}_s^{\min}(\sigma_{i,u}^2)$ attains its minimum value at $\sigma_{i,u}^2=0$. Since γ, σ_s^2, $\sigma_{i,u}^2+\sigma_{i,c}^2$, and σ^2 are fixed, it can be verified that the second term in the bracket of the above equation $-(1+\cos\gamma)^2(2\sigma_{i,c}^2+\sigma_{i,u}^2)/(2\sigma_{i,c}^2+\sigma^2+\sigma_{i,u}^2)$ is an increasing function of $\sigma_{i,u}^2$. Therefore, $\text{SINR}_s^{\min}(\sigma_{i,u}^2)$ is an increasing function of $\sigma_{i,u}^2$, and hence, the minimum of $\text{SINR}_s^{\min}(\sigma_{i,u}^2)$ is attained when $\sigma_{i,u}^2=0$. ∎

APPENDIX C
PROOF OF THEOREM 2

We first establish a lemma.

Lemma C.1: Let $(\phi_1,\psi_1)=(0,0)$ and $\psi_2=0$. Then, we have i) $|\mathbf{a}_{d,2}^H\mathbf{a}_i|^2=(1+\cos\gamma)^2\sin^2(\Delta_i^{d,1}/2)$, and ii) if $\Delta_{d,1}^{d,2}=\pi$, then $\mathbf{a}_{d,2}^H\mathbf{a}_{d,1}=0$, and $\mathbf{a}_{d,2}^H\mathbf{B}_i\mathbf{B}_i^H\mathbf{a}_{d,1}=0$.

Proof of Lemma C.1: Since $\mathbf{B}_{d,2}^H\mathbf{B}_i=(1+\cos\gamma)^2\mathbf{I}_2$, it can be deduced that $|\mathbf{a}_{d,2}^H\mathbf{a}_i|^2=(1+\cos\gamma)^2|\mathbf{h}_{d,2}^H\mathbf{Q}_{d,2}^H\mathbf{Q}_i\mathbf{h}_i|^2$. By Lemma 1, we obtain

$$|\mathbf{a}_{d,2}^H\mathbf{a}_i|^2=(1+\cos\gamma)^2\cos^2\frac{\Delta_i^{d,2}}{2}.\tag{C.1}$$

Now, since $\Delta_{d,1}^{d,2}=\pi$ and $\mathbf{p}_i$ is a point on the arc joining the two points $\mathbf{p}_{d,2}$ and $\mathbf{p}_{d,1}$, we have $\Delta_i^{d,2}=\pi-\Delta_i^{d,1}$. Therefore, (C.1) can be rewritten as

$$|\mathbf{a}_{d,2}^H\mathbf{a}_i|^2=(1+\cos\gamma)^2\sin^2\frac{\Delta_i^{d,1}}{2}.$$

Next, since $\Delta_{d,1}^{d,2}=\pi$, we obtain from Lemma 1 that $\mathbf{h}_{d,2}^H\mathbf{Q}_{d,2}^H\mathbf{Q}_{d,1}\mathbf{h}_{d,1}=0$. Therefore, $\mathbf{a}_{d,2}^H\mathbf{a}_{d,1}=2\mathbf{h}_{d,2}^H\mathbf{Q}_{d,2}^H\mathbf{Q}_{d,1}\mathbf{h}_{d,1}=0$. Moreover, since $\mathbf{B}_{d,2}^H\mathbf{B}_i=(1+\cos\gamma)^2\mathbf{I}_2$, we obtain $\mathbf{a}_{d,2}^H\mathbf{B}_i\mathbf{B}_i^H\mathbf{a}_{d,1}=\mathbf{h}_{d,2}^H\mathbf{Q}_{d,2}^H(\mathbf{B}_{d,2}^H\mathbf{B}_i\mathbf{B}_i^H\mathbf{B}_{d,2})\mathbf{Q}_{d,1}\mathbf{h}_{d,1}=(1+\cos\gamma)^2\mathbf{h}_{d,2}^H\mathbf{Q}_{d,2}^H\mathbf{Q}_{d,1}\mathbf{h}_{d,1}=0$. ∎

Proof of Theorem 2: We shall only establish the expression of $\text{SINR}_{d,1}$ since the expression of $\text{SINR}_{d,2}$ can be obtained with the same technique. We consider two cases that cover all possible scenarios: a) $\sigma_{i,u}^2=0$, and b) $\sigma_{i,u}^2\neq 0$.

Case a) $\sigma_{i,u}^2=0$*:* By Lemma 2, we can express $\text{SINR}_{d,1}$ given in (2.9) as

$$\begin{aligned}\text{SINR}_{d,1}&=\sigma_{d,1}^2\mathbf{a}_{d,1}^H(\mathbf{R}_d-\sigma_{d,1}^2\mathbf{a}_{d,1}\mathbf{a}_{d,1}^H)^{-1}\mathbf{a}_{d,1}\\&=\sigma_{d,1}^2\mathbf{a}_{d,1}^H(\sigma_{d,2}^2\mathbf{a}_{d,2}\mathbf{a}_{d,2}^H+\mathbf{B}_i\mathbf{R}_i\mathbf{B}_i^H\\&\qquad+\sigma^2\mathbf{I}_6)^{-1}\mathbf{a}_{d,1}\\&=\sigma_{d,1}^2\mathbf{a}_{d,1}^H\left[(\mathbf{a}_{d,2}\ \ \mathbf{a}_i)\begin{pmatrix}\sigma_{d,2}^2&0\\0&\sigma_{i,c}^2\end{pmatrix}\begin{pmatrix}\mathbf{a}_{d,2}^H\\\mathbf{a}_i^H\end{pmatrix}\right.\\&\qquad\left.+\sigma^2\mathbf{I}_6\right]^{-1}\mathbf{a}_{d,1}.\end{aligned}$$

Using Lemma A.1 with $\mathbf{W}=\sigma^2\mathbf{I}_6$ and $\mathbf{X}=\mathbf{Y}=(\mathbf{a}_{d,2}\ \ \mathbf{a}_i)\mathbf{C}$, where $\mathbf{C}=\left(\begin{smallmatrix}\sigma_{d,2}&0\\0&\sigma_{i,c}\end{smallmatrix}\right)$, we obtain

$$\begin{aligned}\text{SINR}_{d,1}&=\sigma_{d,1}^2\mathbf{a}_{d,1}^H\left[\frac{1}{\sigma^2}\mathbf{I}_6-\frac{1}{\sigma^4}(\mathbf{a}_{d,2}\ \ \mathbf{a}_i)\mathbf{C}\right.\\&\qquad\times\left(\mathbf{I}_2+\frac{1}{\sigma^2}\mathbf{C}^H\begin{pmatrix}\mathbf{a}_{d,2}^H\\\mathbf{a}_i^H\end{pmatrix}(\mathbf{a}_{d,2}\ \ \mathbf{a}_i)\mathbf{C}\right)^{-1}\\&\qquad\left.\times\mathbf{C}^H\begin{pmatrix}\mathbf{a}_{d,2}^H\\\mathbf{a}_i^H\end{pmatrix}\right]\mathbf{a}_{d,1}\\&=\sigma_{d,1}^2\mathbf{a}_{d,1}^H\left[\frac{1}{\sigma^2}\mathbf{I}_6-\frac{1}{\sigma^4}(\mathbf{a}_{d,2}\ \ \mathbf{a}_i)\left(\begin{pmatrix}\frac{1}{\sigma_{d,2}^2}&0\\0&\frac{1}{\sigma_{i,c}^2}\end{pmatrix}\right.\right.\\&\qquad\left.\left.+\frac{1}{\sigma^2}\begin{pmatrix}2&\mathbf{a}_{d,2}^H\mathbf{a}_i\\\mathbf{a}_i^H\mathbf{a}_{d,2}&2\end{pmatrix}\right)^{-1}\begin{pmatrix}\mathbf{a}_{d,2}^H\\\mathbf{a}_i^H\end{pmatrix}\right]\mathbf{a}_{d,1}.\end{aligned}$$

Since $\mathbf{a}_{d,1}^H\mathbf{a}_{d,1}=2$ and $\mathbf{a}_{d,2}^H\mathbf{a}_{d,1}=0$ (by Lemma C.1), we have

$$\begin{aligned}\text{SINR}_{d,1}&=\sigma_{d,1}^2\left(\frac{2}{\sigma^2}-\frac{1}{\sigma^4}(0\ \ \mathbf{a}_{d,1}^H\mathbf{a}_i)\mathbf{G}\begin{pmatrix}0\\\mathbf{a}_i^H\mathbf{a}_{d,1}\end{pmatrix}\right)\\&=\sigma_{d,1}^2\left(\frac{2}{\sigma^2}-\frac{1}{\sigma^4}\mathbf{a}_{d,1}^H\mathbf{a}_i g\mathbf{a}_i^H\mathbf{a}_{d,1}\right)\\&=\sigma_{d,1}^2\left(\frac{2}{\sigma^2}-\frac{1}{\sigma^4}g\|\mathbf{a}_{d,1}^H\mathbf{a}_i\|^2\right)\end{aligned}\tag{C.2}$$

where

$$\mathbf{G}=\begin{pmatrix}\frac{1}{\sigma_{d,2}^2}+\frac{2}{\sigma^2}&\frac{1}{\sigma^2}\mathbf{a}_{d,2}^H\mathbf{a}_i\\\frac{1}{\sigma^2}\mathbf{a}_i^H\mathbf{a}_{d,2}&\frac{1}{\sigma_{i,c}^2}+\frac{2}{\sigma^2}\end{pmatrix}^{-1}$$

and g is the second-row second-column entry of $\mathbf{G}$. It can be shown that

$$g=\frac{\sigma^2\sigma_{i,c}^2(\sigma^2+2\sigma_{d,2}^2)}{(\sigma^2+2\sigma_{d,2}^2)(\sigma^2+2\sigma_{i,c}^2)-\sigma_{d,2}^2\sigma_{i,c}^2|\mathbf{a}_{d,2}^H\mathbf{a}_i|^2}.\tag{C.3}$$

Since by Lemma A.3, $|\mathbf{a}_{d,1}^H\mathbf{a}_i|^2=(1+\cos\gamma)^2\cos^2(\Delta_i^{d,1}/2)$ and by Lemma C.1, $|\mathbf{a}_{d,2}^H\mathbf{a}_i|^2=(1+\cos\gamma)^2\sin^2(\Delta_i^{d,1}/2)$, we obtain from (C.2) and (C.3) that shown in (C.4), shown at the bottom of the next page, which is equal to the expression of $\text{SINR}_{d,1}$ given in Theorem 2 when $\sigma_{i,u}^2=0$.

Case b) $\sigma_{i,u}^2 \neq 0$: By Lemma 2, we can express $\text{SINR}_{d,1}$ given in (2.9) as

$$\begin{aligned}\text{SINR}_{d,1} &= \sigma_{d,1}^2 \mathbf{a}_{d,1}^H (\mathbf{R}_d - \sigma_{d,1}^2 \mathbf{a}_{d,1}\mathbf{a}_{d,1}^H)^{-1}\mathbf{a}_{d,1} \\ &= \sigma_{d,1}^2 \mathbf{a}_{d,1}^H (\sigma_{d,2}^2 \mathbf{a}_{d,2}\mathbf{a}_{d,2}^H + \mathbf{B}_i\mathbf{R}_i\mathbf{B}_i^H \\ &\qquad + \sigma^2\mathbf{I}_6)^{-1}\mathbf{a}_{d,1} \\ &= \sigma_{d,1}^2 \mathbf{a}_{d,1}^H \left[\sigma^2\mathbf{I}_6 + (\mathbf{a}_{d,2}\mathbf{B}_i)\begin{pmatrix}\sigma_{d,2}^2 & \mathbf{0}_{1\times 2}\\ \mathbf{0}_{2\times 1} & \mathbf{R}_i\end{pmatrix}\right. \\ &\qquad \left.\times \begin{pmatrix}\mathbf{a}_{d,2}^H \\ \mathbf{B}_i^H\end{pmatrix}\right]^{-1}\mathbf{a}_{d,1}.\end{aligned}$$

Since $\sigma_{i,u}^2 \neq 0$, the matrix $\mathbf{R}_i$ is invertible. Now, using Lemma A.1 with $\mathbf{W} = \sigma^2\mathbf{I}_6$ and $\mathbf{X} = \mathbf{Y} = (\mathbf{a}_{d,2}\ \mathbf{B}_i)\mathbf{C}$, where $\mathbf{C}$ is a 3×3 matrix such that $\mathbf{C}\mathbf{C}^H = \left(\begin{smallmatrix}\sigma_{d,2}^2 & \mathbf{0}_{1\times 2}\\ \mathbf{0}_{2\times 1} & \mathbf{R}_i\end{smallmatrix}\right)$, we obtain

$$\begin{aligned}\text{SINR}_{d,1} &= \sigma_{d,1}^2 \mathbf{a}_{d,1}^H \left[\frac{1}{\sigma^2}\mathbf{I}_6 - \frac{1}{\sigma^4}(\mathbf{a}_{d,2}\quad \mathbf{B}_i)\mathbf{C}\right. \\ &\qquad \times \left(\mathbf{I}_3 + \frac{1}{\sigma^2}\mathbf{C}^H\begin{pmatrix}\mathbf{a}_{d,2}^H \\ \mathbf{B}_i^H\end{pmatrix}(\mathbf{a}_{d,2}\quad \mathbf{B}_i)\mathbf{C}\right)^{-1} \\ &\qquad \left.\times\, \mathbf{C}^H\begin{pmatrix}\mathbf{a}_{d,2}^H \\ \mathbf{B}_i^H\end{pmatrix}\right]\mathbf{a}_{d,1} \\ &= \sigma_{d,1}^2 \mathbf{a}_{d,1}^H \left[\frac{1}{\sigma^2}\mathbf{I}_6 - \frac{1}{\sigma^4}(\mathbf{a}_{d,2}\quad \mathbf{B}_i)\right. \\ &\qquad \times \left(\begin{pmatrix}\frac{1}{\sigma_{d,2}^2} & \mathbf{0}_{1\times 2}\\ \mathbf{0}_{2\times 1} & \mathbf{R}_i^{-1}\end{pmatrix} + \frac{1}{\sigma^2}\begin{pmatrix}\mathbf{a}_{d,2}^H \\ \mathbf{B}_i^H\end{pmatrix}(\mathbf{a}_{d,2}\ \mathbf{B}_i)\right)^{-1} \\ &\qquad \left.\times \begin{pmatrix}\mathbf{a}_{d,2}^H \\ \mathbf{B}_i^H\end{pmatrix}\right]\mathbf{a}_{d,1} \\ &= \sigma_{d,1}^2 \mathbf{a}_{d,1}^H \left(\frac{1}{\sigma^2}\mathbf{I}_6 - \frac{1}{\sigma^4}(\mathbf{a}_{d,2}\ \mathbf{B}_i)\mathbf{H}\begin{pmatrix}\mathbf{a}_{d,2}^H \\ \mathbf{B}_i^H\end{pmatrix}\right)\mathbf{a}_{d,1}\end{aligned}$$

where

$$\mathbf{H} = \begin{pmatrix}\frac{1}{\sigma_{d,2}^2} + \frac{2}{\sigma^2} & \frac{1}{\sigma^2}\mathbf{a}_{d,2}^H\mathbf{B}_i \\ \frac{1}{\sigma^2}\mathbf{B}_i^H\mathbf{a}_{d,2} & \mathbf{R}_i^{-1} + \frac{2}{\sigma^2}\mathbf{I}_2\end{pmatrix}^{-1}.$$

Since $\mathbf{a}_{d,1}^H\mathbf{a}_{d,1} = 2$ and by Lemma C.1, $\mathbf{a}_{d,2}^H\mathbf{a}_{d,1} = 0$, we obtain

$$\begin{aligned}\text{SINR}_{d,1} &= \sigma_{d,1}^2\left(\frac{2}{\sigma^2} - \frac{1}{\sigma^4}(0\quad \mathbf{a}_{d,1}^H\mathbf{B}_i)\mathbf{H}\begin{pmatrix}0 \\ \mathbf{B}_i^H\mathbf{a}_{d,1}\end{pmatrix}\right) \\ &= \sigma_{d,1}^2\left(\frac{2}{\sigma^2} - \frac{1}{\sigma^4}\mathbf{a}_{d,1}^H\mathbf{B}_i\tilde{\mathbf{H}}\mathbf{B}_i^H\mathbf{a}_{d,1}\right)\end{aligned}$$

where $\tilde{\mathbf{H}} \in \mathbb{C}^{2\times 2}$ is a submatrix of $\mathbf{H}$ with the first row and the first column being removed. Let $c = 1/\sigma_{d,2}^2 + 2/\sigma^2$, $\mathbf{d} = (1/\sigma^2)\mathbf{B}_i^H\mathbf{a}_{d,2}$, and $\mathbf{D} = (\mathbf{R}_i^{-1} + (2/\sigma^2)\mathbf{I}_2)$. Then, $\mathbf{H}^{-1} = \left(\begin{smallmatrix}c & \mathbf{d}^H\\ \mathbf{d} & \mathbf{D}\end{smallmatrix}\right)$, and it can be verified that

$$\mathbf{H} = \begin{pmatrix}\frac{1}{\delta_1} & -\frac{1}{\delta_1}\mathbf{d}^H\mathbf{D}^{-1} \\ -\frac{1}{\delta_1}\mathbf{D}^{-1}\mathbf{d} & \mathbf{D}^{-1} + \frac{1}{\delta_1}\mathbf{D}^{-1}\mathbf{d}\mathbf{d}^H\mathbf{D}^{-1}\end{pmatrix}$$

where δ_1 is as defined in (4.3). Therefore, we have

$$\tilde{\mathbf{H}} = \mathbf{D}^{-1} + \frac{1}{\delta_1}\mathbf{D}^{-1}\mathbf{d}\mathbf{d}^H\mathbf{D}^{-1}.$$

Now, substituting the expression of $\mathbf{D}^{-1}$ established in Lemma A.2 into $\tilde{\mathbf{H}}$ and using the fact that $\mathbf{a}_{d,2}^H\mathbf{B}_i\mathbf{B}_i^H\mathbf{a}_{d,1} = 0$ established in Lemma C.1, we obtain (after some manipulation)

$$\begin{aligned}\text{SINR}_{d,1} = \sigma_{d,1}^2\left(\frac{2}{\sigma^2} - \frac{1}{\sigma^4}\left(\mu\|\mathbf{a}_{d,1}^H\mathbf{B}_i\|^2 + \nu|\mathbf{a}_{d,1}^H\mathbf{a}_i|^2\right.\right. \\ \left.\left. + \frac{\nu^2}{\sigma^4\delta_1}|\mathbf{a}_{d,1}^H\mathbf{a}_i|^2|\mathbf{a}_{d,2}^H\mathbf{a}_i|^2\right)\right).\end{aligned}$$

Finally, substituting the expressions of $\|\mathbf{a}_{d,1}^H\mathbf{B}_i\|^2$ and $|\mathbf{a}_{d,1}^H\mathbf{a}_i|^2$ established in Lemma A.3 and that of $|\mathbf{a}_{d,2}^H\mathbf{a}_i|^2$ established in Lemma C.1, we obtain (after some manipulation)

$$\begin{aligned}\text{SINR}_{d,1} = \sigma_{d,1}^2\left[\frac{2}{\sigma^2} - \frac{(1+\cos\gamma)^2}{\sigma^4}\left(\mu + \nu\cos^2\frac{\Delta_i^{d,1}}{2}\right.\right. \\ \left.\left. + \frac{\nu^2}{4\sigma^4\delta_1}(1+\cos\gamma)^2\sin^2\Delta_i^{d,1}\right)\right].\end{aligned} \tag{C.5}$$

Combining (C.4) for Case a) and (C.5) for Case b), we obtain the expression of $\text{SINR}_{d,1}$ in Theorem 2. ■

APPENDIX D
PROOF OF COROLLARIES 1–5 OF THEOREM 2

We first establish Corollary 1. Since $\gamma \neq \pi$, we have $(1+\cos\gamma)^2 \neq 0$. Therefore, to show that $\text{SINR}_{d,1}$ is an increasing function of $\Delta_i^{d,1}$, it suffices to show that

$$\nu\cos^2\frac{\Delta_i^{d,1}}{2} + \frac{\nu^2}{4\sigma^4\delta_1}(1+\cos\gamma)^2\sin^2\Delta_i^{d,1}$$

is a decreasing function of $\Delta_i^{d,1}$ since μ is independent of $\Delta_i^{d,1}$. The above expression can be rewritten as

$$\frac{\cos^2\frac{\Delta_i^{d,1}}{2}\,\nu(\sigma^2(\sigma^2+2\sigma_{d,2}^2) - \sigma_{d,2}^2\mu(1+\cos\gamma)^2)}{f(\Delta_i^{d,1})} \tag{D.1}$$

where $f(\Delta_i^{d,1})$ is a function of $\Delta_i^{d,1}$ given by

$$\begin{aligned}f(\Delta_i^{d,1}) = \sigma^2(\sigma^2+2\sigma_{d,2}^2) - \sigma_{d,2}^2(\mu+\nu)(1+\cos\gamma)^2 \\ + \sigma_{d,2}^2\nu(1+\cos\gamma)^2\cos^2\frac{\Delta_i^{d,1}}{2}.\end{aligned}$$

$$\text{SINR}_{d,1} = \frac{\sigma_{d,1}^2}{\sigma^2}\left[2 - \frac{\sigma_{i,c}^2(\sigma^2+2\sigma_{d,2}^2)(1+\cos\gamma)^2\cos^2\frac{\Delta_i^{d,1}}{2}}{(\sigma^2+2\sigma_{d,2}^2)(\sigma^2+2\sigma_{i,c}^2) - \sigma_{d,2}^2\sigma_{i,c}^2(1+\cos\gamma)^2\sin^2\frac{\Delta_i^{d,1}}{2}}\right] \tag{C.4}$$

Since $\nu(\sigma^2(\sigma^2+2\sigma_{d,2}^2)-\sigma_{d,2}^2\mu(1+\cos\gamma)^2)$ is positive and independent of $\Delta_i^{d,1}$, it suffices to establish that $\cos^2(\Delta_i^{d,1}/2)/f(\Delta_i^{d,1})$ is a decreasing function of $\Delta_i^{d,1}$. Now, let us consider $\cos^2(\epsilon_1/2)/f(\epsilon_1)-\cos^2(\epsilon_2/2)/f(\epsilon_2)$, where $\epsilon_1>\epsilon_2\in[0,\pi]$. Then, it can be shown that

$$\begin{aligned}&\frac{\cos^2\frac{\epsilon_1}{2}}{f(\epsilon_1)}-\frac{\cos^2\frac{\epsilon_2}{2}}{f(\epsilon_2)}\\&\quad=\left(\cos^2\frac{\epsilon_1}{2}-\cos^2\frac{\epsilon_2}{2}\right)\times(\sigma^2(\sigma^2+2\sigma_{d,2}^2)\\&\qquad-\sigma_{d,2}^2(\mu+\nu)(1+\cos\gamma)^2)/(f(\epsilon_1)f(\epsilon_2)).\end{aligned}\tag{D.2}$$

Since $(\mu+\nu)=\sigma^2(\sigma_{i,u}^2+2\sigma_{i,c}^2)/2(\sigma^2+\sigma_{i,u}^2+2\sigma_{i,c}^2)<\sigma^2/2$, it can be shown that $f(\epsilon_1)$, $f(\epsilon_2)>0$, and $\sigma^2(\sigma^2+2\sigma_{d,2}^2)-\sigma_{d,2}^2(\mu+\nu)(1+\cos\gamma)^2>0$. Consequently, we obtain from (D.2) that $\cos^2(\epsilon_1/2)/f(\epsilon_1)-\cos^2(\epsilon_2/2)/f(\epsilon_2)<0$ since $\epsilon_1>\epsilon_2$. Therefore, $\cos^2(\Delta_i^{d,1}/2)/f(\Delta_i^{d,1})$ is a decreasing function of $\Delta_i^{d,1}$, and hence, $\mathrm{SINR}_{d,1}$ is an increasing function of $\Delta_i^{d,1}$. Similarly, it can be shown that $\mathrm{SINR}_{d,2}$ is an increasing function of $\Delta_i^{d,2}$. This establishes Corollary 1.

Next, Corollary 2 follows directly from the fact that $(1+\cos\gamma)^2$ is a decreasing function of γ. On the other hand, Corollary 3 is quite obvious. Corollary 4 follows from the fact that $(1+\cos\gamma)^2$ equal to 0 when $\gamma=\pi$ and that μ, $\cos^2(\Delta_i^{d,k}/2)$, and $\sin^2\Delta_i^{d,k}$ are all equal to 0 when $\Delta_i^{d,k}=\pi$ and $\sigma_{i,u}^2=0$ for $k=1,2$.

Next, we shall establish Corollary 5. Consider a fixed DOA separation γ. Since $\sigma_{d,1}^2$, $\sigma_{d,2}^2$, $\sigma_{i,u}^2+\sigma_{i,c}^2$, and σ^2 are fixed, the variables that affect $\mathrm{SINR}_{d,k}$ are $\sigma_{i,u}^2$ (or $\sigma_{i,c}^2$) and $\Delta_i^{d,k}$. By Corollary 1 of Theorem 2, for a given $\sigma_{i,u}^2$, $\mathrm{SINR}_{d,k}$ attains its minimum at $\Delta_i^{d,k}=0$, and moreover, the expression of $\mathrm{SINR}_{d,k}$ is

$$\begin{aligned}\mathrm{SINR}_{d,k}^{\min}(\sigma_{i,u}^2)&=\sigma_{d,k}^2\left(\frac{2}{\sigma^2}-\frac{(1+\cos\gamma)^2(\mu+\nu)}{\sigma}\right)\\&=\sigma_{d,k}^2\left(\frac{2}{\sigma^2}-\frac{(1+\cos\gamma)^2(2\sigma_{i,c}^2+\sigma_{i,u}^2)}{2\sigma_{i,c}^2+\sigma^2+\sigma_{i,u}^2}\right).\end{aligned}\tag{D.3}$$

Now, it remains to be shown that $\mathrm{SINR}_{d,k}^{\min}(\sigma_{i,u}^2)$ attains its minimum at $\sigma_{i,u}^2=0$. Note that the expression of (D.3) is a constant multiple of that of (B.1). Thus, using the technique in the proof of the Corollary 5 of Theorem 1, we can show that $\mathrm{SINR}_{d,k}(\sigma_{i,u}^2)$ attains its minimum when $\sigma_{i,u}^2=0$. ■

ACKNOWLEDGMENT

The authors are grateful to B. Hochwald of Lucent Tecnologies, K.-C. Tan of the Centre for Signal Processing, Singapore, and the reviewers for their useful suggestions.

REFERENCES

[1] A. Nehorai and E. Paldi, "Vector sensor processing for electromagnetic source localization," in *Proc. 25th Asilomar Conf. Signals, Syst. Comput.*, Pacific Grove, CA, Nov. 1991, pp. 566–572.

[2] ——, "Vector-sensor array processing for electromagnetic source localization," *IEEE Trans. Signal Processing*, vol. 42, pp. 376–398, Feb. 1994.

[3] K.-C. Tan, K.-C. Ho, and A. Nehorai, "Uniqueness study of measurements obtainable with arrays of electromagnetic vector sensors," *IEEE Trans. Signal Processing*, vol. 44, pp. 1036–1039, Apr. 1996.

[4] ——, "Linear independence of steering vectors of an electromagnetic vector sensor," *IEEE Trans. Signal Processing*, vol. 44, pp. 3099–3107, Dec. 1996.

[5] K.-C. Ho, K.-C. Tan, and W. Ser, "An investigation on number of signals whose directions-of-arrival are uniquely determinable with an electromagnetic vector sensor," *Signal Process.*, vol. 47, no. 1, pp. 41–54, Nov. 1995.

[6] B. Hochwald and A. Nehorai, "Identifiability in array processing models with vector-sensor applications," *IEEE Trans. Signal Processing*, vol. 44, pp. 83–95, Jan. 1996.

[7] K.-C. Ho, K.-C. Tan, and B. T. G. Tan, "Efficient method for estimating directions-of-arrival of partially polarized signals with electromagnetic vector sensors," *IEEE Trans. Signal Processing*, vol. 45, pp. 2485–2498, Oct. 1997.

[8] ——, "Estimation of directions-of-arrival of partially polarized signals with electromagnetic vector sensors," in *Proc. ICASSP*, May 1996, vol. 5, pp. 2900–2903.

[9] K.-C. Ho, K.-C. Tan, and A. Nehorai, "Estimation of directions-of-arrival of completely polarized and incompletely polarized signals with electromagnetic vector sensors," in *Proc. 11th IFAC Symp. Syst. Ident.*, Kitakyushu City, Japan, July 1997, vol. 2, pp. 523–528.

[10] J. Li, "Direction and polarization estimation using arrays with small loops and short dipoles," *IEEE Trans. Antennas Propagat.*, vol. 41, pp. 379–387, Mar. 1993.

[11] K. T. Wong and M. D. Zoltowski, "High accuracy 2D angle estimation with extended aperture vector sensor arrays," in *Proc. ICASSP*, May 1996, vol. 5, pp. 2789–2792.

[12] ——, "Uni-vector-sensor ESPRIT for multi-source Azimuth-elevation angle-estimation," in *Proc. IEEE Antennas Propagat. Soc., APS Int. Symp. Dig.*, 1996, vol. 2, pp. 1368–1371.

[13] M. D. Zoltowski and K. T. Wong, "Polarization diversity & extended-aperture spatial diversity to mitigate fading-channel effects with a sparse array of electric dipoles or magnetic loops," in *Proc. IEEE Int. Veh. Technol. Conf.*, 1997, pp. 1163–1167.

[14] K. T. Wong and M. D. Zoltowski, "Self-initiating MUSIC-based direction finding in polarization beamspace," in *IEE Radar Conf.*, 1997.

[15] B. Hochwald and A. Nehorai, "Polarimetric modeling and parameter estimation with applications to remote sensing," *IEEE Trans. Signal Processing*, vol. 43, pp. 1923–1935, Aug. 1995.

[16] G. F. Hatke, "Conditions for unambiguous source localization using polarization diverse arrays," in *Proc. 27th Asilomar Conf. Signals, Syst. Comput.*, Los Alamitos, CA, 1993, pp. 1365–1369.

[17] ——, "Performance analysis of the superCART antenna array," MIT Lincoln Lab., Lexington, MA, Project Rep. AST-22, Mar. 1992.

[18] B. D. Van Veen and K. M. Buckley, "Beamforming: A versatile approach to spatial filtering," *IEEE Acoust. Speech, Signal Processing Mag.*, vol. 5, pp. 4–24, Apr. 1988.

[19] Y. Hua, "A pencil-MUSIC algorithm for finding two-dimensional angles and polarization using cross dipoles," *IEEE Trans. Antennas Propagat.*, vol. 41, pp. 370–376, Mar. 1993.

[20] Q. Cheng and Y. Hua, "Performance analysis of the MUSIC and pencil-MUSIC algorithms for diversely-polarized arrays," *IEEE Trans. Signal Processing*, vol. 42, pp. 3150–3165, Nov. 1994.

[21] ——, "Further study of the pencil-MUSIC algorithm for estimating two-dimensional angles," *IEEE Trans. Aerosp. Electron. Syst.*, vol. 32, pp. 284–299, Jan. 1996.

[22] R. T. Compton, Jr., "The tripole antenna: An adaptive array with full polarization flexibility," *IEEE Trans. Antennas Propagat.*, vol. AP-29, pp. 944–952, Nov. 1981.

[23] M. Kanda, "An electromagnetic near-field sensor for simultaneous electric and magnetic-field measurements," *IEEE Trans. Electromagn. Compat.*, vol. EMC–26, pp. 102–110, Aug. 1984.

[24] M. Kanda and D. Hill, "A three-loop method for determining the radiation characteristics of an electrically small source," *IEEE Trans. Electromagn. Compat.*, vol. 34, pp. 1–3, Feb. 1992.

[25] K.-C. Tan and Z. Goh, "A detailed derivation of arrays free of higher rank ambiguities," *IEEE Trans. Signal Processing*, vol. 44, pp. 351–359, Feb. 1996.

[26] R. A. Monzingo and T. W. Miller, *Introduction to Adaptive Arrays.* New York: Wiley, 1980.

[27] G. A. Deschamps, "Geometrical representation of the polarization of a plane electromagnetic wave," *Proc. IEEE*, vol. 55, pp. 2143–2159, Dec. 1967.

[28] H. Cox, "Resolving power and sensitivity to mismatch of optimum array processors," *J. Acoust. Soc. Amer.*, vol. 54, pp. 771–785, 1973.

[29] L. C. Godara and A. Cantoni, "Uniqueness and linear independence of steering vectors in array space," *J. Acoust. Soc. Amer.*, vol. 70, no. 2, pp. 467–475, Aug. 1981.
[30] A. Nehorai, K.-C. Ho, and B. T. G. Tan, "Minimum-noise-variance beamformer with an electromagnetic vector sensor," Dept. Elect. Eng. Comput. Sci., Univ. Illinois, Chicago, Rep. UIC-EECS-97-3, Apr. 1997.
[31] B. A. Cray and A. H. Nuttall, "A comparison of vector-sensing and scalar-sensing linear arrays," Naval Undersea Warfare Center Div., Newport, RI, NUWC-NPT Tech. Rep. 10632, Jan. 1997.
[32] M. A. Hawkes and A. Nehorai, "Acoustic vector-sensor beamforming and Capon direction estimation," *IEEE Trans. Signal Processing*, vol. 46, pp. 2291–2304, Sept. 1998.
[33] G. H. Golub and C. F. Van Loan, *Matrix Computations.* Baltimore, MD: Johns Hopkins Univ. Press, 1983.

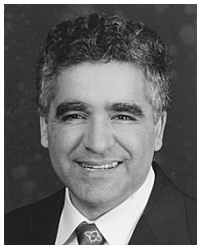

Arye Nehorai (S'80–M'83–SM'90–F'94) received the B.Sc. and M.Sc. degrees in electrical engineering from the Technion—Israel Institute of Technology, Haifa, in 1976 and 1979, respectively, and the Ph.D. degree in electrical engineering from Stanford University, Stanford, CA, in 1983.

After graduation, he became a Research Engineer at Systems Control Technology, Inc., Palo Alto, CA. From 1985 to 1995, he was with the Department of Electrical Engineering, Yale University, New Haven, CT, where he became an Associate Professor in 1989. In 1995, he joined the Department of Electrical Engineering and Computer Science at The University of Illinois, Chicago (UIC), as a Full Professor. He holds a joint professorship with the Bioengineering Department at UIC.

Dr. Nehorai is an Associate Editor of the IEEE TRANSACTIONS ON ANTENNAS AND PROPAGATION, the IEEE JOURNAL OF OCEANIC ENGINEERING, of *Circuits, Systems, and Signal Processing*, and of *The Journal of the Franklin Institute* and has been an Associate Editor of the IEEE TRANSACTIONS ON ACOUSTICS, SPEECH, AND SIGNAL PROCESSING. He served as Chairman of the Connecticut IEEE Signal Processing Chapter from 1986 to 1995 and is currently Vice Chair of the IEEE Signal Processing Society's Technical Committee on Sensor Array and Multichannel (SAM) Processing. He was co-recipient, with P. Stoica, of the 1989 IEEE Signal Processing Society's Senior Award for Best Paper. He has been a Fellow of the Royal Statistical Society since 1996.

Kwok-Chiang Ho was born in Singapore in 1968. He received the B.Sc. degree (with honors) in mathematics from the National University of Singapore in 1993.

From 1993 to 1996, he worked at the Defence Science Organization of the Ministry of Defence, Singapore, as an Analyst. Since August 1996, he has been working at the Centre for Signal Processing, Nanyang Technological University, as a Project Officer. His research interests are in array signal processing, speech processing, and digital communications.

B. T. G. Tan received the B.Sc. degree (with honors) in physics from the University of Singapore in 1965 and the D.Phil. degree from Oxford University, Oxford, U.K., in 1968.

Since 1968, he has taught at the National University of Singapore, where he is now an Associate Professor in Physics. His research interests include the microwave properties of semiconductors and dielectrics, surface physics, image processing, and digital sound synthesis.

Dr. Tan is a chartered engineer and a member of the Institution of Electrical Engineers.